Running head: **Zinc homeostasis in *A. halleri* and *A. thaliana***

Manuscript Draft

Corresponding author:

Ute Krämer
Max Planck Institute of Molecular Plant Physiology
Am Mühlenberg 1,
D-14476 Golm
Germany
Tel.: +49 (331) 5678 357
FAX: +49 (331) 5678 98 357
Email: kraemer@mpimp-golm.mpg.de

Genetics, Genomics, and Molecular Evolution – Associate Editor Thomas Mitchell-Olds

Title:

Zn-dependent global transcriptional control, transcriptional de-regulation and higher gene copy number for genes in metal homeostasis of the hyperaccumulator *Arabidopsis halleri*[1]

Ina N. Talke[2], Marc Hanikenne[2] and Ute Krämer[*]

Max Planck Institute of Molecular Plant Physiology, D-14476 Potsdam-Golm, Germany

[1] This work was supported by the Deutsche Forschungsgemeinschaft (Kr 1967/3), the European Union (Research Training Network *METALHOME*, HPRN-CT-2002-00243), the German Federal Ministry of Education and Research (Biofuture 0311877), and the Max Planck Institute of Molecular Plant Physiology.

[2] These authors contributed equally to the manuscript.

[*] Corresponding author; e-mail kraemer@mpimp-golm.mpg.de; fax +49 331 5678 408

Abstract

The metal hyperaccumulator *Arabidopsis halleri* exhibits naturally selected Zn and Cd hypertolerance and accumulates extraordinarily high Zn concentrations in its leaves. With these extreme physiological traits, *A. halleri* phylogenetically belongs to the sister clade of *A. thaliana*. Using a combination of genome-wide cross-species microarray analysis and real-time RT-PCR, a set of candidate genes is identified for Zn hyperaccumulation, Zn and Cd hypertolerance, and the adjustment of micronutrient homeostasis in *A. halleri*. Eighteen putative metal homeostasis genes are newly identified to be more highly expressed in *A. halleri* than in *A. thaliana*, and 11 previously identified candidate genes are confirmed. The encoded proteins include HMA4 known to contribute to root-shoot transport of Zn in *A. thaliana*. Expression of either AtHMA4 or AhHMA4 confers cellular Zn and Cd tolerance to *Saccharomyces cerevisiae*. Among further newly implicated proteins are IRT3 and ZIP10, which have been proposed to contribute to cytoplasmic Zn influx, and FRD3 required for iron partitioning in *A. thaliana*. In *A. halleri*, the presence of more than a single genomic copy is a hallmark of several highly expressed candidate genes with possible roles in metal hyperaccumulation and metal hypertolerance. Both *A. halleri* and *A. thaliana* exert tight regulatory control over Zn homeostasis at the transcript level. Zn hyperaccumulation in *A. halleri* involves enhanced partitioning of Zn from roots into shoots. The transcriptional regulation of marker genes suggests that in the steady-state, *A. halleri* roots – but not the shoots – act as physiologically Zn deficient under conditions of moderate Zn supply.

Introduction

Metal hyperaccumulation is a rare trait found in approximately 440 plant taxa, 11 of which have been reported to hyperaccumulate Zn (Reeves and Baker, 2000). Individuals of these taxa accumulate very high Zn concentrations of more than 10,000 μg g^{-1} Zn in leaf dry biomass (Baker and Brooks, 1989). The accumulation of higher metal concentrations in shoots than in roots has been described as a characteristic of hyperaccumulation in both hydroponic and soil culture (Baker et al., 1994; Krämer et al., 1996; Weber et al., 2004). All known metal hyperaccumulator taxa occur primarily on geologically metal-rich or metal-contaminated soils and possess extraordinarily high metal tolerance. The number of Zn and Ni hyperaccumulator taxa is higher in the Brassicaceae family than in any other plant family, and includes a large number of Ni hyperaccumulator species in the section Odontarrhena of the genus *Alyssum* and the two most commonly studied Zn hyperaccumulator model species *Thlaspi caerulescens* and *Arabidopsis halleri* (Reeves and Baker, 2000).

Both subspecies of *Arabidopsis halleri*, ssp. *gemmifera* and ssp. *halleri*, are hyperaccumulators of Zn, and ssp. *halleri* is able to grow healthily and to accumulate very high leaf Zn concentrations of between 3000 and 22,000 μg g^{-1} dry biomass within a wide dynamic range of external Zn concentrations in the field (Bert et al., 2000; Dahmani-Muller et al., 2000; Kubota and Takenaka, 2003). The leaves of individuals of some populations have additionally been reported to contain hyperaccumulator levels of Cd of more than 100 μg g^{-1} dry biomass (Dahmani-Muller et al., 2000). Together, *A. halleri* and its non-accumulating close relative *A. lyrata* form the sister clade of *A. thaliana* (Koch et al., 2000; Yogeeswaran et al., 2005). *A. halleri* and *A. thaliana* share on average approximately 94% nucleotide sequence identity within coding regions (Becher et al., 2004). Leaves of both *A. lyrata* and *A. thaliana* commonly accumulate between 40 and 80 μg g^{-1} Zn, and gradually develop chlorosis when they contain significantly higher metal concentrations (Macnair et al., 1999; Desbrosses-Fonrouge et al., 2005). In hydroponic culture, the growth of *A. halleri* roots has been reported to tolerate at least 30-fold higher Zn and 10-fold higher Cd concentrations than root growth of *A. lyrata* (Macnair et al., 1999; Bert et al., 2003). These observations illustrate the dramatic alterations in metal homeostasis of *A. halleri* compared to both *A. thaliana* and *A. lyrata*, despite a very close phylogenetic relationship and high overall sequence conservation among these three species (Clemens et al., 2002; Krämer and Clemens, 2005).

Researchers have begun to address the major differences between the metal homeostasis networks of closely related metal hyperaccumulator and non-accumulator plants at the molecular level (Salt

and Krämer, 2000; Clemens et al., 2002; Krämer and Clemens, 2005). Using single-gene and transcriptomic approaches, the most notable differences observed in hyperaccumulator compared to closely related non-accumulators plants were high relative transcript levels of several candidate genes (Pence et al., 2000; Assunção et al., 2001; Becher et al., 2004; Dräger et al., 2004; Papoyan and Kochian, 2004; Weber et al., 2004; Hammond et al., 2006; Mirouze et al., 2006). Differences in the functions of hyperaccumulator candidate gene products, when compared to their *A. thaliana* orthologues, have not extensively been documented so far (Bernard et al., 2004; Roosens et al., 2004).

The observed high transcript levels of candidate genes in *A. halleri* and in other hyperaccumulator model plants are based on a modified regulation of transcript levels (Pence et al., 2000; Becher et al., 2004; Weber et al., 2004). This could involve at least four possible mechanisms. Firstly, it is conceivable that for some *A. halleri* genes, the presence or activity of proximal *cis* elements or *trans* factors controlling transcript levels could be altered in comparison to *A. thaliana*. Secondly, it is possible that the affinity of a Zn sensing machinery that down-regulates transcript levels encoding Zn acquisitory proteins may be reduced in *A. halleri*. Thirdly, Zn requirement of *A. halleri* may merely be higher than in closely related non-accumulator plants. Finally, the high expression of a specific gene of *A. halleri* could be an indirect consequence of another alteration in a different element of the metal homeostasis network, which is complex and tightly regulated in plants. Before dissecting the molecular basis underlying the modified regulation of expression of individual candidate genes in *A. halleri*, it is therefore important to understand globally how the regulation of the metal homeostasis network is altered.

For *A. halleri MTP1*, which is involved in Zn hypertolerance, the amplification of gene copy number contributes to enhanced *MTP1* transcript levels, when compared to *A. thaliana* or *A. lyrata* (Dräger et al., 2004). It has not been investigated whether genomic copy number is also increased for other genes involved in naturally selected metal hyperaccumulation or hypertolerance of *A. halleri*.

Previously, root and shoot transcript profiles were established in separate studies using *A. halleri* and *A. thaliana* grown under different conditions and Affymetrix 8K chips representing only a limited number of genes (Becher et al., 2004; Weber et al., 2004). To obtain a comprehensive account of directly comparable expression profiles for both roots and shoots of the two species, we employed the next generation of Affymetrix Arabidopsis GeneChips, the ATH1 microarray, covering more than 22,500 genes.

Here we present genome-wide transcriptional profiles of hydroponically cultivated *A. halleri* and *A. thaliana* plants maintained under control conditions or upon a short-term exposure to high Zn

concentrations. We report a set of candidate genes for metal hyperaccumulation and tolerance, the adjustment of micronutrient homeostasis and the protection from secondary abiotic stress in *A. halleri*. For several of the most highly expressed candidate genes, genomic copy number is estimated to be higher in *A. halleri* than in *A. thaliana* by DNA gel blot. The detailed analysis of transcriptional regulation of candidate genes by real-time RT-PCR is combined with existing and newly generated knowledge on gene product function to develop a model of the alterations in the metal homeostasis network underlying metal hyperaccumulation in *A. halleri*.

Results

Establishment of experimental conditions

To compare the effect of external Zn supply on Zn accumulation and partitioning in *A. thaliana* and *A. halleri*, plants were cultivated hydroponically and supplied with different sub-toxic Zn concentrations for 3 weeks (Figures 1 A and 1 B). In *A. halleri*, the ratio of shoot Zn concentrations to root Zn concentrations was above unity in plants cultivated in a Zn-deficient hydroponic solution containing no added Zn for 3 weeks (Figure 1 C). Continuous supply of Zn concentrations of between 1 and 5 µM led to an increase in the shoot:root ratio of Zn concentrations, with maximum ratios approximately tripling the ratio determined under Zn-deficient conditions. By contrast, *A. thaliana* partitioned into the shoots only a small proportion of the Zn concentration accumulated in the roots (Fig. 1 A, B). This was reflected in shoot:root Zn concentration ratios substantially below unity, which decreased further with increasing Zn supply (Fig. 1 C). When *A. halleri* was cultivated in media containing high Zn concentrations of 30 µM or 300 µM Zn, shoot:root ratios of Zn concentrations were below unity and only about one-quarter of the ratios measured at 0.3 µM Zn. These results indicated that *A. halleri* accumulates Zn predominantly in the shoot even at very low Zn supply, whereas *A. thaliana* primarily immobilizes Zn in the roots irrespective of the Zn supply. In addition to the dramatic inter-species differences in Zn partitioning between roots and shoots, the data suggest a species-specific modulation of Zn partitioning dependent on the Zn supply.

To select suitable conditions and time points for transcript profiling, transcript levels of three metal homeostasis genes, *ZIP4* , *ZIP9* and *NAS2*, were determined in preliminary experiments (Figure 2). These genes are known to be Zn-responsive at the transcript level in *A. thaliana* (Grotz et al., 1998; Wintz et al., 2003), and they have previously been identified as candidate genes for Zn accumulation and tolerance in *A. halleri* (Becher et al., 2004; Weber et al., 2004).

Plants of two different Zn steady-states were subjected to short-term increases in external Zn supply. In one experiment, plants grown under control (1 μM) Zn conditions were exposed to excess Zn concentrations of 30 μM Zn for *A. thaliana* and 300 μM Zn for *A. halleri*, for 2 and 8 h[1]. The choice of concentrations reflects naturally selected Zn tolerance in *A. halleri*, whereas *A. thaliana* possesses only basic Zn tolerance (Clemens, 2001; Becher et al., 2004). In an additional experiment, Zn-deficient plants cultivated in a medium lacking added Zn for 3 weeks were re-supplied with a Zn concentration of 5 μM (Fig. 2).

In roots, Zn-induced changes in transcript levels were observed as early as 2 h after increasing the Zn concentrations in the hydroponic medium (Fig. 2, upper row: *ZIP4*, *ZIP9*). In shoots, transcriptional responses were observed 2 or 8 h after the increase in Zn concentrations in the hydroponic medium (Fig. 2, bottom row: *ZIP4*, *ZIP9* and *NAS2*). Transcripts of *ZIP9* encoding a transporter of the ZIP family and *NAS2* encoding a nicotianamine synthase were not detectable in shoots of either *Arabidopsis* species grown in the presence of sufficient (control) Zn, but were strongly induced upon Zn deficiency (Fig. 2, *ZIP9*, *NAS2*). This suggested that neither of the two species experienced Zn deficiency under the chosen control conditions.

Comparison of A. *halleri* and *A. thaliana* transcript profiles with ATH1 GeneChips

According to the results from the preliminary experiments, microarrays were hybridized with labeled cRNAs prepared from roots and shoots of *A. halleri* and *A. thaliana* grown at 1 μM Zn and after 2 h and 8 h of exposure to excess Zn for roots and shoots, respectively (see Materials and Methods). Under control conditions, higher signal intensities were detected for a total of 628 probe sets in roots, and for 1739 probe sets in shoots of *A. halleri* compared to *A. thaliana* (as outlined in Materials and Methods; for visualization see all colored, non-grey datapoints in Figure 3 A and B; complete gene lists with annotations in Supplemental Tables I and II). We also identified genes which responded at the transcript level to excess Zn in *A. halleri* (see Materials and Methods, Supplemental Tables III and IV). In order to group the identified genes according to functional classes, a genome-wide annotation list was assembled; this list includes the class of metal homeostasis-related genes, which contained all functionally characterized *A. thaliana* genes encoding proteins involved in metal transport, chelation, binding and trafficking and all other members of the respective protein families, and genes encoding members of protein families known to participate in metal homeostasis in other organisms (Supplemental Table XI: class "Metal ion homeostasis", Fig. 3, see Materials and Methods). The intersection of the gene list of metal

[1] In preliminary experiments, the chosen concentrations were the maximum Zn concentrations that did not cause a reduction in biomass gain in *A. thaliana* and *A. halleri*, respectively, during 4 d of exposure (Martina Becher, Ina N. Talke, Agnes N. Chardonnens and Ute Krämer, unpublished data).

homeostasis-related genes and of the genes which are either more highly expressed (Supplemental Tables I and II) or Zn-regulated in *A. halleri* (Supplemental Tables III and IV) contained a total of 17 genes in the roots and 19 genes in the shoots, with 7 genes in common between both roots and shoots (Fig. 3; Table I). We considered these genes as an initial set of major candidate genes for an involvement in naturally selected metal tolerance and hyperaccumulation in *A. halleri*.

The metal homeostasis genes newly identified here as candidate genes encode proteins encompassing both cellular functions known to be of primary importance in metal homeostasis: membrane transport of metals and metal binding/chelation. The 12 new candidate genes encoding proteins that are likely to be involved in the transport of Zn or other metals across membranes were *ZIP10* (zinc-regulated transporter/iron-regulated transporter-like protein 10, roots, 111-fold), *MTP8* (metal tolerance protein 8, shoots, 65-fold), *HMA4* (heavy metal associated domain-containing protein 4, or heavy metal ATPase 4, shoots, 53-fold), *FRD3* (ferric reductase defective 3, roots, 45-fold), *PHT1;4* (phosphate transporter 1;4, roots, 19-fold), *CHX18* (cation/H^+ exchanger 18, roots, 6.5-fold), *MTP11* (shoots, 4.7-fold), *HMA6*/*PAA1* (P-type ATPase from *Arabidopsis thaliana*, shoots, 4.6-fold), *IREG2* (iron-regulated transporter 1, roots, 4.5-fold), *IRT3* (iron-regulated transporter 3, roots, 4.5-fold), *YSL6* (yellow-stripe 1-like protein 6, shoots, 4.4-fold), and *ZIP3* (downregulated 2.7-fold in roots following exposure to excess Zn) (Fristedt et al., 1999; Curie et al., 2001; Mäser et al., 2001; Rogers and Guerinot, 2002; Blaudez et al., 2003; Jensen et al., 2003; Lahner et al., 2003; Shikanai et al., 2003; Green and Rogers, 2004; Hussain et al., 2004; Shin et al., 2004). A total of 5 new candidate genes encoding metal-binding proteins or proteins involved in the biosynthesis of metal chelators included *FER2* (ferritin 2, shoots, 11-fold), *SAMS1* (S-adenosylmethionine synthetase 1, shoots, 10-fold), *SAMS2* (shoots, 8.5-fold), *FER1* (ferritin 1, shoots, 5.1-fold), and *SAMS3* (roots and shoots, around 5-fold) (Peleman et al., 1989; Petit et al., 2001). The compound S-adenosylmethionine is the substrate for nicotianamine synthase, and the *A. halleri* nicotianamine synthase genes *NAS2* and *NAS3* have previously been implicated in Zn tolerance of *A. halleri* (Becher et al., 2004; Weber et al., 2004) (see also Table I).

Two additional, closely related genes encoding the protein disulfide isomerases 1 and 2 were included among the set of candidate genes analyzed here because of their interesting regulation and potential function in metal detoxification (*PDI1*: shoots, 39-fold higher in *A. halleri*; *PDI2*: shoots, 17-fold; Table I) (Rensing et al., 1997; Narindrasorasak et al., 2003). These proteins are the closest sequence relatives of a previously characterized ER-localized protein from castor bean, which catalyzes the isomerization of disulfide bridges within proteins. Enhanced PDI activity is thought to

protect plants from stress that results in the modification of SH groups of ER proteins (Houston et al., 2005).

Microarray analysis of Zn-dependent transcriptional regulation

Among candidate genes, the microarray data suggested a trend towards decreasing transcript levels in response to excess Zn in roots of both *A. thaliana* and *A. halleri* (Table I). Conversely, in *A. halleri* roots transcript levels of *ZIP* and *NAS* genes were increased under Zn deficiency, when compared to control conditions (Table I). In shoots of *A. thaliana*, transcript levels of several candidate genes were increased in response to excess Zn, namely for *PDI* and *SAMS* genes, and for *YSL6* (Table I). In *A. halleri*, transcript levels of these genes were constitutively high and unchanged in response to excess Zn (Table I). Our data suggested that, especially in shoots, *A. halleri* responds differently to excess Zn than *A. thaliana* at the transcript level.

We investigated whether the species-specific patterns observed in metal-dependent transcriptional regulation of candidate genes are also reflected globally across the entire panel of genes represented on the ATH1 microarray. In roots of *A. halleri* and *A. thaliana*, exposure to excess Zn resulted in increased transcript levels for 0.5% and 0.9%, respectively, of all expressed genes, and in decreased transcript levels for only 0.09% and 0.07%, respectively, of all expressed genes (Supplemental Tables III and V, $P < 0.1$). Thus, the predominant directions of transcriptional responses to excess Zn were identical in roots of *A. halleri* and *A. thaliana*, with a global trend towards upregulation opposing a trend towards downregulation among our set of candidate genes in both species. In shoots of *A. thaliana*, among all expressed genes, transcriptional upregulation was observed in response to excess Zn (0% down, 3.2% up, $P < 0.1$, Supplemental Table VI). By comparison, in shoots of *A. halleri* a smaller proportion of expressed genes responded, and transcriptional downregulation was predominant (0.8% down, 0.2% up, $P < 0.1$; Supplemental Table IV). This indicated that primarily in the shoots the two species respond differently to excess Zn also at the whole transcriptome level.

Confirmation of candidate genes by real-time RT-PCR

To assess the reliability of the cross-species expression differences between *A. halleri* and *A. thaliana* detected using the microarrays, we determined transcript levels by an alternative method, quantitative real-time RT-PCR, for a subset of 18 genes (Table II). Overall, there was good qualitative agreement between the ratios of microarray signals in *A. halleri* relative to *A. thaliana* and the ratios of transcript levels as determined by real-time RT-PCR (Table II). The false negatives

according to microarray hybridization, *ZIP3* and *HMA4* (in roots), could be attributed to a high divergence of the *A. halleri* sequence from the *A. thaliana* sequence in the region covered by the oligonucleotide probes on the microarray, in combination with a modest magnitude of the *A. halleri* : *A. thaliana* ratio of transcript levels. For several other genes, quantitative discrepancies between microarray and real-time RT-PCR data are likely to be attributable to cross-hybridization between high transcript levels of a gene in *A. halleri* and the probes for a closely related member of the same gene family (*NAS2* on *NAS4* in roots, *NAS3* on *NAS2* in shoots, *NAS2* on *NAS3* in shoots under Zn deficiency, *PDI1* on *PDI2*). It was reported earlier that very low signals (for example, for *ZIP10*, *MTP8*, *ZIP9* in *A. thaliana*) are often quantified imprecisely on the ATH1 chip (Czechowski et al., 2004), and for these genes in particular, the real-time RT-PCR results are likely to be more accurate.

Functional analysis of the novel candidate protein AhHMA4

Out of all candidate genes identified here, absolute transcript levels were highest for *A. halleri HMA4* (see Table II), which encodes a membrane transport protein of the P_{1B} transition metal pump family of the P-type ATPases (Axelsen and Palmgren, 2001). To determine the cellular function of this candidate gene, which had not previously been implicated in metal hyperaccumulation or metal tolerance in *A. halleri*, we expressed AhHMA4 and AtHMA4 in metal hypersensitive mutants of budding yeast (*Saccharomyces cerevisiae*) (Figure 4). Both the *A. thaliana* and the *A. halleri* HMA4 proteins were similarly able to complement Zn hypersensitivity of the *zrc1 cot1* double mutant and Cd hypersensitivity of the *ycf1* mutant of *Saccharomyces cerevisiae* (Fig. 4 A and B). When the transport functions of AtHMA4 and AhHMA4 were disrupted by converting the conserved aspartate residues (D401) of the phosphorylation motifs (Axelsen and Palmgren, 2001) into alanines, respectively, complementation was no longer observed. Consequently, Zn and Cd are substrates of both Arabidopsis HMA4 proteins in yeast, and the observed complementation is attributable to the transport functions of the proteins and not to the known ability of the cytoplasmic C-termini of AtHMA4 and related proteins to bind metal ions (Bernard et al., 2004; Papoyan and Kochian, 2004).

Gene copy number of highly expressed candidate genes in *A. halleri*

Previously, high transcript levels of the Zn tolerance gene *MTP1* were partly attributed to the presence of several *MTP1* gene copies in the genome of *A. halleri*, whereas the genome of the closely related non-tolerant species *A. thaliana* contains only a single *MTP1* gene copy (Dräger et

al., 2004). To estimate the genomic copy number for other candidate genes in *A. halleri*, we generated genomic DNA blots for 12 of these genes (Kim et al., 1998; Marquardt et al., 2000; Small and Wendel, 2000; Ishizaki et al., 2002). Complex band patterns suggested that more than one gene copy is present in the *A. halleri* genome for the genes *ZIP3*, *ZIP6*, *ZIP9* and *HMA4* (Figure 5 A to D, Table III, Supplemental Figure 1, for data evaluation see also Materials and Methods). For comparison, the maximum expression of these genes was 8-fold, 10-fold, 13-fold and 30-fold higher in *A. halleri* than in *A. thaliana*, respectively, as determined by real-time RT-PCR (Table II). By contrast, the simple band patterns of the genomic DNA blots indicated that a number of other candidate genes are most likely to be present as single copies in the *A. halleri* genome. These include *FRD3*, *ZIP4*, *MTP8*, *ZIP10*, *IRT3*, *PHT1;4* and *PDI1,* the maximum expression of which was 16-fold, 12-fold, 11-fold, 6-fold, 5-fold, 5-fold and 4-fold in *A. halleri* compared to *A. thaliana*, respectively (Tables II, III, Fig. 5). Among the group of candidate genes for which DNA gel blot analysis was performed, more than single gene copies were detected for each of the three candidate genes exhibiting the highest transcript levels in *A. halleri* (normalized to *EF1α* transcript levels), i.e., *HMA4* and *ZIP9* and *ZIP3* (compare Table II, left part). Based on sequence data and restriction analysis of genomic PCR products (see Table 3), it is unlikely that additional bands on the DNA gel blots originated from uncharacterized restriction sites rather than additional gene copies in the *A. halleri* genome.

Regulation of candidate gene expression

Transcriptional Zn responses were further investigated for a subset of 18 candidate genes using real-time RT-PCR (Figure 6). In the roots of *A. halleri*, short term exposure to 300 µM Zn for 2 and 8 h resulted in the downregulation of transcript levels of a group of genes, which encode several ZIP family Zn transporters with likely functions in Zn influx into the cytoplasm (Fig. 6 A). Downregulation of transcript levels of this group of genes was clearly less pronounced in the roots of *A. thaliana* after short-term exposure to 30 µM Zn. It has to be kept in mind that in roots of *A. halleri* the Zn-induced decrease in transcript levels occurs from very high transcript levels under control conditions. Consequently, despite a more pronounced downregulation in *A. halleri*, final root transcript levels 8 h after supply of excess Zn were generally higher in *A. halleri* than in *A. thaliana* (compare Fig. 2).

Different from roots, shoot transcript levels of most *ZIP* genes were generally as low in *A. halleri* as in *A. thaliana* under control conditions (see Fig. 2, Table II). In shoots of *A. halleri*, there was virtually no transcriptional response to a short-term oversupply of Zn, whereas *A. thaliana* shoots responded by a marked downregulation of several genes including primarily *ZIP* genes and *PHT1;4*

(Fig. 6 B). In order to test whether the shoots of *A. halleri* were able to respond transcriptionally to changes in Zn supply, we investigated gene expression under Zn deficiency (Fig. 6). Zn deficiency resulted in a very pronounced increase in shoot transcript levels of genes encoding ZIP family transporters and nicotianamine synthase proteins (Fig. 6 B, see Table 1). In roots of *A. halleri*, Zn deficiency resulted in a moderate increase in transcript levels of these genes, when compared to the high transcript levels observed under control conditions (Fig. 6 A; for comparison with *A. thaliana*, see Figs. 2 and 7).

To analyze the specificity of transcriptional Zn responses, candidate gene regulation in *A. halleri* was also investigated following exposure to moderate excesses of Cd (30 µM) or Cu (5 µM) and NaCl (100 mM) for 2 h and 8 h (Fig. 6). The results suggested that overall, Zn responses were rather specific. Some of the Zn-responsive genes, primarily *NAS* and *ZIP* genes, were also downregulated in response to excess Cu, as for excess Zn. The transcriptional responses to excess Zn and excess Cd, however, were distinct. Furthermore, there was a second group of genes exhibiting a pattern of regulation that was clearly different from the Zn- and Cu-repressed genes. Expression of these genes was induced in response to exposure to 100 mM NaCl and included *MTP8*, *PHT1;4*, *FRD3*, *ZIP6* and *OASA2*. Transcript levels of subsets of these genes were also increased following exposure to excess Cu or Cd, supporting their responsiveness to abiotic stress. *PDI* transcript levels showed few changes over the entire range of conditions, with an increase in root *PDI2* transcript levels in response to excess Cu in *A. halleri* and an increase in *PDI1* transcript levels in response to Zn in shoots of *A. thaliana*.

Transcript levels of *HMA4* appeared to be constitutively very high in the roots of *A. halleri* across all treatments, and only slightly induced under Zn deficiency in *A. halleri* shoots (Fig. 6 A, B). A detailed analysis confirmed the extremely high expression of *HMA4* in roots and shoots of *A. halleri* (Figure 7). Under Zn-deficiency, shoot *HMA4* transcript levels were slightly increased, and they were reduced to control levels shortly after re-addition of Zn to the medium (Fig. 7).

We investigated transcript levels of the additional newly identified candidate genes *ZIP3* and *IRT3*, under different conditions of Zn deficiency, re-supply and oversupply (Fig. 7). There were overall similarities in short-term Zn responses of plants maintained under control (1 µM added Zn) and Zn-deficient (0 µM added Zn) conditions (Fig. 7, see also Fig. 2). In response to re-supply of 5 µM Zn to Zn-deficient plants, there was a decrease in transcript levels for these Zn-deficiency-induced genes in both *A. halleri* and *A. thaliana*. In roots of *A. halleri*, after the initial downregulation, which was strongest 2 h after re-supply of Zn, a general trend of a gradual increase in transcript levels was observed at later time points (Fig. 7). This demonstrated clearly that there is no general

defect in the magnitude or time scale of transcriptional Zn responses in *A. halleri* (Fig. 7, see also Fig. 2: *ZIP4* and *ZIP9* in controls and at time points 8 h and 24 h).

Discussion

In a microarray-based cross-species comparative transcript analysis in *A. thaliana* and *A. halleri*, we identified a set of candidate genes expressed at higher levels in *A. halleri* than in *A. thaliana* or regulated by Zn in *A. halleri* (Figure 3, Table I, Supplemental Tables I to IV). Microarray data were confirmed by an alternative technique of transcript quantification, real-time RT-PCR, for a representative subset of genes. Among the genes identified using microarrays, combined *in silico* and real-time RT-PCR analyses revealed a total of 29 genes encoding putative metal homeostasis proteins, which we consider here as an initial set of major candidates for a role in naturally selected metal hyperaccumulation and associated metal hypertolerance in *A. halleri*. Of these, 18 genes have not previously been implicated in these traits, and 11 confirm earlier findings (Table I, II) (Becher et al., 2004; Weber et al., 2004; Mirouze et al., 2006).

We performed DNA gel blots to estimate genomic copy numbers for a subset of 12 candidate genes (Figure 5, Table III, Supplemental Fig. 1). The obtained data are important for future studies of segregation of candidate genes and for the cloning of genomic sequences from *A. halleri*. Moreover, the combination of DNA gel blot with steady-state transcript level data suggested the presence of more than a single genomic copy in *A. halleri* of the genes, for which the highest transcript levels were detected, *HMA4*, *ZIP9* and *ZIP3* (Tables II, III). As reported previously for *MTP1* (Dräger et al., 2004), an increased gene copy number of these genes may contribute to the ability of *A. halleri* to express these genes at very high levels, and possibly allows for regulatory diversification among the copies of these genes. However, high expression of these candidate genes cannot be explained without additionally invoking an altered regulation of transcript levels. Moreover, substantially higher transcript levels in *A. halleri* than in *A. thaliana*, as also found for *FRD3*, *ZIP4* and *MTP8*, were not in all cases associated with indications for more than a single genomic copy of the respective candidate gene.

Ratios of shoot:root Zn concentrations are generally below unity in *A. thaliana* and other non-accumulator plants, and typically above unity in *A. halleri* and other Zn hyperaccumulating plants (Baker et al., 1994; Dahmani-Muller et al., 2000; Becher et al., 2004; Weber et al., 2004) (Fig. 1). Zn concentrations partitioned into shoots relative to the roots were dependent on the external Zn supply (Fig. 1). In addition, the adjustment of Zn partitioning as a function of Zn supply differed between *A. thaliana* and *A. halleri*, with maximum relative Zn concentrations partitioned into the shoot at approximately 5 µM in *A. halleri*, and under Zn deficiency in *A. thaliana*. In *A. halleri* the partitioning of Zn into the shoot was restricted at high external Zn supply of 30 µM Zn and above. This may contribute to Zn hypertolerance in the Langelsheim accession of *A. halleri*. It has been reported that individuals from the most Zn-hypertolerant populations of *A. halleri*, which include the Langelsheim accession, accumulate lower leaf Zn concentrations than individuals from less hypertolerant populations (Bert et al., 2000; Bert et al., 2002). As expected based on Zn partitioning, we observed between-species differences in gene expression under control conditions, as well as species-specific short-term transcriptional Zn responses of candidate genes in *A. halleri* and *A. thaliana* (Tables I, II, Figs. 1, 2, 6, 7).

Transcript levels of genes known to be transcriptionally regulated by Zn, such as *ZIP1*, *ZIP3*, *ZIP4*, *ZIP9*, *NAS2* and *NAS3* can be used as indicators of the Zn *status* of Arabidopsis plants (Grotz et al., 1998; Wintz et al., 2003). The expression of a group of Zn deficiency marker genes suggested that both roots and shoots of *A. thaliana* are largely Zn-sufficient at 1 or 5 µM Zn, and concertedly experience Zn deficiency after prolonged growth in a medium lacking added Zn (Figs. 2, 7). Similarly, the expression of the same set of genes in *A. halleri* plants grown at 1 or 5 µM Zn suggests that the shoots are Zn-sufficient under these conditions (see *NAS2*, *ZIP9* and *ZIP4* transcript levels in shoots in Fig. 2, Figs. 6, 7). By contrast, the roots of *A. halleri* act transcriptionally as Zn-deficient after prolonged growth at 1 or 5 µM Zn. Thus, transcript levels of a common set of Zn *status* marker genes can be interpreted to indicate that roots and shoots of *A. halleri* experience different Zn *stati* in the steady state.

There was a rapid and strong downregulation of transcript levels of *ZIP3*, *ZIP4* and *IRT3* in roots of *A. halleri* following exposure to excess Zn or re-supply of Zn to roots of Zn-deficient plants grown in a medium lacking added Zn (Figs. 2, 7). Overall, this suggests that short-term Zn-dependent downregulation of Zn deficiency-induced transcripts in roots of *A. halleri* is generally as functional and efficient as in *A. thaliana*. Only *NAS2* and *ZIP9* transcript levels were not or only partly Zn-responsive in roots of *A. halleri*, respectively. The Zn-dependent control of transcript abundance of these two genes in *A. thaliana* appears to be partially or fully inactive in roots, but not in shoots, of *A. halleri*. The simplest explanation for the high expression of Zn deficiency responsive genes in

the roots of *A. halleri* at normal Zn supplies could be a loss of Zn from the roots *via* high root-to-shoot Zn transport rates (see Fig. 1). The proteins encoded by two of the candidate genes have been implicated in root-to-shoot metal translocation in *A. thaliana*: HMA4 and FRD3.

The *A. thaliana* HMA4 protein is a P_{1B}-type metal pump that localizes to the plasma membrane and mediates cellular metal efflux. Together with the related AtHMA2, AtHMA4 has a role in the transport of Zn from the root to the shoot and in metal detoxification (Hussain et al., 2004; Verret et al., 2004; Mills et al., 2005). According to real-time RT-PCR analysis (Fig. 7, Table II), *HMA4* transcript levels are between 4- and 10-fold higher in roots and at least 30-fold higher in shoots of *A. halleri* than in *A. thaliana*. In *A. halleri*, *HMA2* transcript levels are much lower than *HMA4* transcript levels (less than 0.25% in shoots and less than 0.2% in roots), and *HMA2* transcript levels are lower in *A. halleri* than in *A. thaliana* (approximately 25% in shoots and 8% in roots; Ina N. Talke, Leonard Krall and Ute Krämer, unpublished quantitative real-time RT-PCR results). Heterologous expression in yeast indicated that AhHMA4 and AtHMA4 are similarly able to complement Zn and Cd hypersensitivity of yeast mutants (Fig. 4), and that complementation is dependent on the transport functions of the proteins. Together, our data suggest that AhHMA4 is functionally highly similar to AtHMA4, and that *HMA4* expression is very high in *A. halleri* and predominant over the expression of *HMA2*. Thus, in the context of the data published on AtHMA4, the data presented here implicate *A. halleri* HMA4 in Zn and Cd hypertolerance and in Zn hyperaccumulation, i.e., the partitioning of Zn predominantly to the shoot.

The *A. thaliana* and *A. halleri* FRD3 proteins are members of the MATE (multi-drug and toxin efflux) family of membrane transport proteins. Although the transport function of AtFRD3 has not yet been directly established, the available data suggest that AtFRD3 has a role in maintaining iron mobility between the root and the shoot. In the *frd3* mutant, root iron deficiency responses are constitutively active, leading to secondary accumulation of a number of metals including Mn, Co, Cu, Zn and Fe in both roots and shoots (Delhaize, 1996; Rogers and Guerinot, 2002; Lahner et al., 2003; Green and Rogers, 2004). Based on published data, one may thus expect *FRD3* to be expressed at low levels in hyperaccumulator plants. Unexpectedly however, *FRD3* is expressed at very high levels in *A. halleri* (Tables I and II, Fig. 6). In agreement with this, Zn hyperaccumulation in *A. halleri* is specific both in terms of the accumulated metal and in terms of the accumulating tissue, which is the shoot (Becher et al., 2004). In addition, Zn accumulation is highest in the vacuoles of leaf mesophyll cells in *A. halleri* (Küpper et al., 2000; Sarret et al., 2002), whereas in the *A. thaliana frd3* mutant Fe and Mn appear to accumulate in the leaf apoplast (Green and Rogers,

2004). In conclusion, based on the available evidence, it can be hypothesized that the high expression of *FRD3* in *A. halleri* contributes to metal homeostasis, but not specifically to the high accumulation of Zn in shoots of *A. halleri*.

In addition to *FRD3*, several other genes found to be highly expressed in *A. halleri* (Table I) were previously associated not with Zn or Cd homeostasis, but with the homeostasis of other transition metals, among them *FER1* (Fe), *FER2* (Fe), *NRAMP3* (Fe, Mn), *IREG2* (Fe), *HMA6*/*PAA1* (Cu), *MTP8* and *MTP11* (Mn) (Thomine et al., 2000; Petit et al., 2001; Delhaize et al., 2003; Shikanai et al., 2003; Thomine et al., 2003; McKie and Barlow, 2004; Lanquar et al., 2005). The encoded proteins may contribute to the tolerance and hyperaccumulation phenotypes by adjusting the homeostasis of Fe, Mn and Cu to the alterations in Zn and Cd homeostasis of *A. halleri*. Alternatively, these proteins may have direct roles in Zn or Cd homeostasis. It will be important to establish the functions of the proteins encoded by these genes in the future.

To address the specificity of Zn-dependent regulation of candidate gene transcript levels, we exposed plants to an excess of Cu, Cd or NaCl in the hydroponic medium. Root *ZIP3* and *ZIP4* transcript levels and transcript levels of all 4 *NAS* genes were suppressed following exposure of *A. halleri* to excess Cu (Fig. 6). Wintz et al. (2003) demonstrated that expression of *A. thaliana* ZIP4 can complement the Cu uptake defect of the *ctr1* yeast mutant. AtZIP3-dependent uptake of $^{65}Zn^{2+}$ into yeast cells was decreased by more than 55% in the presence of a ten-fold excess of $CuCl_2$ (Grotz et al., 1998). Root-to-shoot transport of Cu in the xylem is likely to occur as a Cu-nicotianamine complex (Pich et al., 1994; Pich and Scholz, 1996; von Wiren et al., 1999). The Cu-induced downregulation of *ZIP* and *NAS* transcript levels observed here in *A. halleri* (Fig. 6) may constitute a regulatory response counteracting excessive Cu uptake and transport to the shoot. Based on the chemical similarity between Cd^{2+} and Zn^{2+} ions, Cd toxicity may involve the disruption of plant Zn homeostasis. However, none of the *ZIP* or *NAS* genes known to have a role in Zn acquisition and distribution were regulated in response to an excess of Cd (Fig. 6). This may reflect the Cd hypertolerance of *A. halleri* (Bert et al., 2003).

There appear to be similarities between major candidate genes expressed at high levels in *A. halleri* and in the metal-tolerant Zn and Cd hyperaccumulator model species *Thlaspi caerulescens*. The *A. halleri* / *A. lyrata* clade is phylogenetically closest to *A. thaliana*, with an estimated divergence time of between 3.5 and 5.8 million years ago (Koch et al., 2001; Yogeeswaran et al., 2005). For comparison, *Thlaspi caerulescens* belongs to the clade containing *Sinapis alba*, which is thought to have diverged from the *A. thaliana* lineage more than 20 million years ago (Gao et al., 2005). In

contrast to *A. halleri*, multiple genomic copies have not been reported for any *T. caerulescens* candidate genes so far. High transcript levels have been observed for *T. caerulescens ZNT1* (Lasat et al., 2000; Pence et al., 2000; Assunção et al., 2001) as well as for its sequence orthologue *AhZIP4* (Becher et al., 2004), and for *TcZNT2* (Assunção et al., 2001) and its sequence orthologue *AhIRT3* (Fig. 7), all of which encode cellular Zn uptake systems. The sequence-orthologous *TcZTP1* (Assunção et al., 2001), *Thlaspi goesingense MTP1* (Persans et al., 2001) and *AhMTP1* transcripts (Becher et al., 2004; Dräger et al., 2004) have all been reported to occur at very high levels in the respective species and encode proteins mediating metal efflux from the cytoplasm. Finally, high transcript levels have been reported for *TcHMA4* (Bernard et al., 2004; Papoyan and Kochian, 2004) and *AhHMA4* (Fig. 7), and the encoded proteins are capable of mediating cellular Zn and Cd detoxification (see Fig. 4; Papoyan and Kochian, 2004). These observations raise the question of whether metal hyperaccumulation and metal hypertolerance are ancestral traits that have subsequently been lost in the majority of Brassicaceae species. We favour the alternative hypothesis that Zn hyperaccumulation evolved several times independently in the Brassicaceae through recent mutations leading to the convergent overexpression of an overlapping set of genes responsible for the Zn hyperaccumulation and hypertolerance traits.

The comprehensive identification of candidate genes in several hyperaccumulator model plants is a prerequisite for their functional, regulatory and sequence analysis. This will be an important step towards a better understanding of the evolution of naturally selected metal hyperaccumulation and associated metal hypertolerance, and of evolutionary genome dynamics in plants. Furthermore, this will allow a comparison with extreme traits in other Arabidopsis relative model systems, such as Na tolerance in *Thellungiella halophila* (Inan et al., 2004; Taji et al., 2004; Gong et al., 2005).

In summary, we have used cross-species transcript profiling to successfully identify on a genome-wide scale a number of candidate genes for naturally selected metal tolerance and hyperaccumulation in *A. halleri*. By exploring candidate genes at the genome, functional and regulatory level we have obtained insights into the complex molecular basis of an extreme physiological trait.

Materials and Methods

Plant material, growth conditions and experimental treatments

Plants of *A. thaliana* (L.) Heynhold (accession Columbia) and *A. halleri* (L.) O'Kane and Al-Shehbaz ssp. *halleri* (accession Langelsheim) were grown from seeds, which were the progeny of a single mother plant in a pool of six individuals grown in an open greenhouse from seeds collected at Langelsheim. Plants were cultivated in hydroponic culture as described in Becher et al. (2004), with a photoperiod of 11 h light, 13 h dark, at a photon flux density 145 µmol m^2 s^{-1} during the day, and day and night temperatures of 20ºC and 18ºC, respectively. In all experiments, each culture vessel of 400 mL hydroponic solution contained three individual plants, and all treatments were harvested at the same time. Experiments for subsequent RNA extraction were harvested by carefully separating roots and shoots of plants, pooling tissues according to treatment, and freezing in liquid nitrogen. Harvested tissues were stored at -80°C until further processing.

Short-term high Zn, Cd, Cu and Na treatments were initiated when plants were 6.5 weeks old. For short-term high Zn supply, the medium was replaced with fresh control medium (1 µM $ZnSO_4$) 8 h before harvest. Then nothing (controls) or 30 µM $ZnSO_4$ and 300 µM $ZnSO_4$ for *A. thaliana* and *A. halleri*, respectively, was added to the hydroponic solution 8 h or 2 h before harvest. Three biologically independent experiments, each comprising five culture vessels per treatment (15 plants per treatment) were conducted. In experiments with Cd, Cu and Na treatments of *A. halleri*, media were exchanged (1 µM $ZnSO_4$; Cd: none; Cu: 0.5 µM $CuSO_4$; Na: 0.1 µM Na_2MO_4) 3 days before harvest; 30 µM $CdCl_2$, 5 µM $CuSO_4$ or 100 mM NaCl were added as treatments 8 h or 2 h before harvest. Two biologically independent experiments were conducted, with at least two culture vessels (at least 6 plants in total) for each treatment.

For Zn deficiency experiments with Zn resupply, the treatment was initiated when plants were 4.5 weeks old and lasted for 3 weeks. For deficiency, $ZnSO_4$ was omitted from the hydroponic solution; the sufficient control solution contained 5 µM $ZnSO_4$. The last change of medium was done 3 days before harvest. For Zn resupply, 5 µM $ZnSO_4$ was added to the hydroponic solution of Zn-deficient plants 24 h, 8 h and 2 h before harvest. Two biologically independent experiments were conducted, each comprising at least three culture vessels (at least 9 plants) per treatment.

In the experiments conducted to determine root and shoot Zn concentrations after long-term treatment with a range of different Zn supplies, plants were 4.5 weeks old when treatments were initiated. For *A. halleri*, the hydroponic solution contained 0, 0.3, 1, 5, 10, 30 or 300 µM $ZnSO_4$, for *A. thaliana* 0, 1, 5 or 10 µM $ZnSO_4$. Upon harvest after 3 weeks of treatment, shoots were briefly rinsed in ultrapure H_2O and blotted dry, and roots from three individuals of the same species and hydroponic culture vessel were desorbed together in 150 mL of an ice-cold solution of 5 mM $CaCl_2$ and 1 mM MES-KOH (pH 5.7) for 20 min, with a replacement of the solution after 5 min, followed by two washes in 150 mL ice-cold water, each for 3 min. Tissues were pooled by culture vessel and

dried at 60°C for 3 days. Two biologically independent experiments were conducted, each comprising three culture vessels (9 plants) per treatment.

Determination of Zn concentrations

Dried root and shoot material was homogenized, and for each sample, 35 to 70 mg were processed and elemental contents analysed by inductively coupled plasma optical emission spectroscopy using an IRIS Advantage Duo ER/S (Thermo Jarrell Ash, Franklin, MA, USA) as described previously (Becher et al., 2004).

RNA extraction

For microarray expression profiling, total RNA was extracted with Trizol (Invitrogen Life Technologies, Karlsruhe, Germany) according to the manufacturer's instructions. RNeasy spin columns and the RNase-free DNase set for on-column DNase digest (Qiagen, Hilden, Germany) were used according to the manufacturer's instructions for subsequent RNA purification and digestion of genomic DNA, and as an alternative method of total RNA isolation when transcript levels were determined by real-time RT-PCR only (RNeasy plant mini kit and RNase-free DNase set; Qiagen). Quality and quantity of RNA was checked visually by denaturing gel electrophoresis and by photometric analysis (absorbance at 260 nm and 280 nm).

Microarray expression profiling and data analysis

Synthesis of cDNA, cRNA labelling, and the hybridization on the GeneChip Arabidopsis ATH1 genome array were done as recommended by the manufacturer (Affymetrix UK Ltd.; manual 701025 rev 1, https://www.affymetrix.com/support/downloads/manuals/expression_s2_manual.pdf). In short, 20 µg of total RNA were used for first-strand cDNA synthesis with 100 pmol $T7(dT)_{24}$ primers and SuperScript II RT (Invitrogen), second-strand cDNA synthesis was carried out with *E. coli* DNA ligase, DNA polymerase I and RNase H (all Invitrogen). Biotin-labelled cRNAs were synthesized by *in vitro* transcription using the Enzo BioArray HighYield RNA transcript labelling kit (Enzo Diagnostics, Inc., Farmingdale, NY, USA). Labelled cRNAs were quantified according to Affymetrix instructions, and a corrected amount of 25 µg cRNA were fragmented in fragmentation buffer (200 mM Tris-acetate, pH 8.1, 500 mM KOAc, 150 mM MgOAc). Before hybridization on ATH1 arrays, sample quality was assessed by hybridization on the test3-array (Affymetrix) for examination of 3'-5' intensity ratios of houskeeping genes. ATH1 GeneChips were hybridized with cRNA from the following experiments: of the short-term Zn supply experiments, two for each treatment, tissue and species; of the Zn deficiency experiments, one for each tissue from the 5 µM

Zn (sufficient) and 0 µM Zn (deficient) treatment, respectively (Dr. F. Wagner, Resource Center and Primary Database, Berlin, Germany).

The microarray suite software package (MAS 5.0, Affymetrix) was used to generate probe set signals of the scanned ATH1 arrays. At a target intensity of 100, scaling factors for arrays hybridized with cRNA from *A. halleri* were on average two-fold higher than scaling factors for *A. thaliana* arrays (*A. halleri*: 0.943 ± 0.196; *A. thaliana*: 0.424 ± 0.093). The arithmetic means of signal intensities over all probe sets were 146.9 ± 8.3 for *A. halleri* and 135.4 ± 9.6 for *A. thaliana*. For *A. thaliana* an average of 13,907 (61.0%) and 11,646 (51.1%) of the total number of 22,810 probe sets were assigned a "present call" by the MAS 5.0 software in roots and shoots, respectively. On average 9750 (42.8%) and 9389 (41.2%) probe sets were assigned a "present call" in roots and shoots, respectively, for *A. halleri*. Pivot data of each hybridized ATH1 GeneChip containing raw signal values and present, marginal and absent calls (flags) were imported from MAS 5.0 into GeneSpring GX (v 7.2; Agilent Technologies, Waldbrunn, Germany; http://www.chem.agilent.com/). Within GeneSpring, the following normalization steps were carried out for each chip: first, signals below 0.01 were set to 0.01; second, all signals within a dataset were normalized to the 50th percentile of the measurements of the chip, using only measurements with a raw signal of at least 12.5; third, in a "per gene" normalization, the signal for each probe set was normalized to the respective signal of the control chip (from the same experiment; chips from *A. thaliana* for inter-species comparisons, control condition for within-species comparisons). Calculation of mean values for raw and normalized signals, statistical analysis and data filtering were performed in GeneSpring. For *A. halleri vs*. *A. thaliana* comparisons, the following filters were applied sequentially to identify genes more highly expressed in *A. halleri* than in *A. thaliana* ("value filter"). First, in order to avoid the identification of false positives in a cross-species evaluation, probe sets were selected that exhibited an at least four-fold higher mean normalized signal in *A. halleri* than in *A. thaliana*. Second, among these probe sets, we selected probe sets for which the mean raw signal value was above 25 in *A. halleri*. Third, we selected only those probe sets, for which in a one sample Student's *t*-test the *P*-value was below 0.05, with false discovery rate (FDR) control adjusted at 5% (Benjamini and Hochberg, 1995). Fourth, only those probe sets were retained, which were assigned at least one "present call" for *A. halleri* among the chips under comparison. For within-species comparisons, to identify genes upregulated and/or downregulated upon exposure to Zn, the following selection criteria were employed sequentially: For upregulation/downregulation in the experimental Zn condition (2 h or 8 h high Zn supply; Zn deficiency), probe sets with (1) a mean normalized signal at least two-fold higher/lower than in the control condition, (2) a mean raw signal above a threshold value (25 for *A. halleri*, 12.5 for *A. thaliana*) and (3) present calls in all biological replicates of the experimental condition

(upregulation)/control condition (downregulation). To obtain an estimate of the percentage of genes regulated in within-species comparisons (as reported in the Results), a *P*-value cutoff of 0.1 was applied. The same cutoff was used for the gene lists shown in Supplemental Tables III, IV and V. The P-value cutoffs were 0.1 for upregulation and 0.2 for downregulation for the gene lists shown in Supplemental Table VI, and 0.05 for upregulation and 0.4 for downregulation for Supplemental Tables VII and VIII.

Lists of candidate probe sets and their respective signal data were exported from GeneSpring. Tables for assigning Affymetrix ATH1 probe set identifiers to Arabidopsis Genome Initiative (AGI) locus identifiers were obtained from TAIR (The Arabidopsis Information Resource; http://www.arabidopsis.org) and GABI (Genomanalyse im biologischen System Pflanze; http://gabi.rzpd.de/services/Affymetrix.shtml). In cases where an ATH1 probe set could not be assigned to one single locus identifier, all locus identifiers represented by this probe set and its associated signal data are given. Annotation and classification of genes as metal ion homeostasis-related, metal ion (Zn, Fe, Cu, Mn) binding, membrane and transport-associated, oxidative stress protection-associated, pathogen response-related and RNA metabolism-associated was done through literature review, keyword searches in TAIR, use of the PlantsT database (http://plantst.genomics.purdue.edu/), and using MapMan annotation based on TAIR5 (Usadel et al., 2005) (http://gabi.rzpd.de/projects/MapMan/). Annotation of genes was obtained from TAIR. Table associations were done with Microsoft Access. In all Tables and Supplemental Tables, *P*-values are given as exported from the program GeneSpring GX, i.e., from a one sample student's *t*-test and not adjusted for FDR.

Real-time RT-PCR

Synthesis of cDNA, primer design and quality control were done as described in Becher et al. (2004). Primer sequences are given in Supplemental Table IX.

Real-time RT-PCR (qPCR) reactions were performed in 384-well plates with an Applied Biosystems ABI Prism 7900HT Sequence Detection System (SDS; Applied Biosystems, Foster City, CA, USA; http://www.appliedbiosystems.com/), using SYBR Green to monitor cDNA amplification. Equal amounts of cDNA, corresponding to approximately 0.06 ng of mRNA were used in each qPCR reaction. In addition, a qPCR reaction contained 5 µL of qPCR mastermix (Applied Biosystems) and 2.5 pmol of forward and reverse primers (Eurogentec, Liège, Belgium) in a total volume of 10 µL. The following standard thermal profile was used: 2 min at 50°C, 10 min at 95°C, 40 repeats of 15 sec at 95°C and 60 sec at 60°C, and a final stage of 15 sec at 95°C, 15 sec at 60°C and 15 sec at 95°C to determine dissociation curves of the amplified products. Data were analyzed using 7900 HT SDS software (v 2.2.1, Applied Biosystems). Threshold cycle (C_T) values

were determined for each reaction at a threshold value of the normalized reporter R_n of 0.2. Furthermore, the reaction efficiency (RE) was determined for each qPCR reaction with LinRegPCR v 7.5 (Ramakers et al., 2003). Real-time RT-PCR was performed on material from at least two independent biological experiments. For confirmation of microarray data we used material from one experiment used for microarray hybdridization and from at least one additional independent experiment not used for microarray hybridization. At least two technical repeats were done for each combination of cDNA and primer pair, and the quality of the qPCR reactions was checked through analysis of the dissociation and amplification curves. Only those reactions were used for data evaluation for which transcripts were reliably detectable (C_T values below 35), and RE was above 1.5. Mean reaction efficiencies (RE_m) were determined for each primer pair and for each *Arabidopsis* species from all qPCR reactions passing the quality control (at least 40 reactions; Supplemental Table IX). Mean C_T values ($C_{T,m}$) were calculated from all quality-checked technical repeats of a cDNA-primer pair combination.

Over all cDNAs used, the average C_T value for the constitutively expressed control gene, elongation factor *EF1*α (At5g60390, Becher et al., 2004), was 18.68 with a standard deviation of 1.03 (n = 76). Transcript levels of genes of interest (GI) within a cDNA were normalized to the respective transcript level of *EF1*α using the following formula:

Relative transcript level, RTL (GI) = $[RE_m\ (EF1\alpha)]^{\ C_{T,m}\ (EF1\alpha)}$ x $[RE_m\ (GI)]^{\ -\ C_{T,m}\ (GI)}$. For clarity, values shown in Tables and Figures are RTL x 10^3.

Cloning

All cloning and molecular biology procedures were carried out according to standard protocols unless indicated otherwise (Sambrook and Russel, 2001). For the candidate genes, *A. halleri* cDNA fragments were amplified with Red-Taq DNA polymerase (Sigma, St. Louis, MO, USA) using primers designed on the basis of the corresponding *A. thaliana* sequences (Supplemental Table X). The standard PCR program was as follows: 3 min at 95 °C, followed by 35 cycles of 30 sec at 95 °C, 30 sec at 55 °C, 1 min per kBp at 72°C and a final extension step of 7 min at 72°C. The PCR products were cloned into the pCR2.1 TOPO vector (Invitrogen, Carlsbad, CA, USA) and the inserts of at least three independent plasmids were sequenced. Unless stated otherwise, *A. halleri*-cDNA-derived probes for DNA gel blot hybridizations were prepared from pCR2.1 TOPO clones by excision of fragments using *Eco*RI. For *ZIP3*, *ZIP6*, *PHT1;4* and *MTP8*, a 472 bp *Hind*III-*Sal*I fragment, a 380 bp *Eco*RI-*Nde*I fragment, a 550 bp *Eco*RI fragment and a 594 bp *Hind*III fragment was used, respectively.

Full length cDNAs for *AtHMA4* and *AhHMA4* were obtained as follows. cDNA libraries were prepared from mRNA of *A. thaliana* (Col-0 accession) inflorescence tissues and from root tissues of

several individuals of *A. halleri* (Langelsheim accession), respectively, using the SMART™ RACE cDNA amplification kit according to the manufacturer's instructions (BD Biosciences, San Jose, CA, USA). The open-reading frames of *AtHMA4* and *AhHMA4* were subsequently amplified using a proofreading polymerase (Pfu Turbo; Stratagene, La Jolla, CA, USA) and the following PCR program: 3 min at 95 °C, followed by 10 cycles of 30 sec at 95 °C, 30 sec at 58 °C, 8 min at 68 °C, 20 cycles of 30 sec at 95 °C, 30 sec at 55 °C, 8 min at 68 °C, and a final extension step of 7 min at 68 °C. The products were cloned directionally into the GATEWAY entry vector pENTR TOPO (Invitrogen), and later subcloned into the yeast centromeric expression vector pFL38H-GW by site-directed recombination according to the manufacturer's instructions (Invitrogen). pFL38H-GW was constructed by inserting a *Sma*I-*Bgl*II fragment from the vector pFL61-AKT1 (Sentenac et al., 1992) into the *Sma*I-*Bgl*II-digested vector pFL38 (Bonneaud et al., 1991), followed by replacement of the *URA3* marker with the *HIS3* marker, which was obtained from YDpH using *Bam*HI, and inserted into the pFL38-derived vector following digestion with *Bgl*II. Subsequently, *AKT1* was excised from the resulting vector using *Not*I, the linearized vector blunt-ended using the Klenow fragment of DNA polymerase I, and a blunt Gateway cassette inserted according to the manufacturer's instructions (Invitrogen). To construct the *AtHMA4* D401A and *AhHMA4* D401A mutant cDNAs, linear amplification was performed of the *AtHMA4* and *AhHMA4* in the yeast expression vector pFL38H-GW in a PCR reaction using mutagenic primers (Supplemental Table X) (12 cycles of 95 °C for 30 sec, 55 °C for 60 sec, 68 °C for 16 min), followed by digestion of the parent DNA with *Dpn*I, and subsequent transformation of *E. coli*. Constructs were verified by sequencing.

Yeast complementation assays

The following yeast strains were used in the assay: *zrc1 cot1* (*Mat a*, *zrc1::natMX3*, *cot1::kan-MX4*, *his3Δ1*, *leu2Δ0*, *met15Δ0*, *ura3Δ0*) (Becher et al., 2004) and its parental strain BY4741 (*Mat a*, *his3Δ1*, *leu2Δ0*, *met15Δ0*, *ura3Δ0*), *ycf1* (*Mat α*; *his3Δ1*; *leu2Δ0*; *lys2Δ0*; *ura3Δ0*; *YDR135c::kanMX4*) and its parental strain BY4742 (*Mat α*; *his3Δ1*; *leu2Δ0*; *lys2Δ0*; *ura3Δ0*) (http://web.uni-frankfurt.de/fb15/mikro/euroscarf/index.html). Preparation of competent cells and transformations were carried out following the polyethylene glycol method (Dohmen et al., 1991). Both yeast mutant strains were transformed with pFL38H-GW empty vector (ev) or pFL38H containing *AtHMA4* and *AhHMA4*, *AtHMA4* D401A and *AhHMA4* D401A cDNAs. As control, the corresponding wild-type strains were transformed with pFL38H-GW empty vector. Transformants were selected and maintained on synthetic complete medium (SC) lacking histidine and with D-glucose as a carbon source. For complementation assays, transformants were grown overnight in 5 mL SC –His media to early stationary phase (OD_{600} approximately 1.0). Yeast cells were then

washed twice with modified low sulphate/phosphate (LSP) medium (Conklin et al., 1992), which contained 80 mM NH_4Cl, 0.5 mM KH_2PO_4, 2mM $MgSO_4$, 0.1 mM $CaCl_2$, 2 mM NaCl, 10 mM KCl, trace elements, vitamins and supplements –His as in SC, 2% (w/v) D-glucose, and serially diluted to identical OD_{600}. Five microliters of each serial dilution were spotted onto LSP –His plates (1.5% agarose, Seakem, BMA, Rockland, ME, USA) containing various concentrations of $ZnSO_4$ (2 μM for controls and between 100 and 400 μM for experimental treatments) or $CdSO_4$ (15 to 60 μM). Results are from one transformant representative of at least three independent transformants for each experiment and two independent experiments.

DNA gel blot analysis

Genomic DNA of *A. thaliana* (Col-0 accession) and clones of two *A. halleri* individuals (Lan 3-1 and Lan 5) of the Langelsheim accession (Ernst, 1974) was isolated as described previously (Dräger et al., 2004). Five micrograms of genomic DNA were digested with 50 U *Eco*RI, *Hind*III or *Nco*I in the appropriate buffer (Roche, Mannheim, Germany), supplemented with 100 μg mL^{-1} bovine casein (Sigma), overnight at 37°C and separated on a 0.9% (w/v) TRIS-acetate-EDTA agarose gel. The DNA was transferred onto an uncharged nylon membrane (Hybond N; Amersham Biosciences, Piscataway, NJ, USA) and cross-linked with UV light at 120 mJ (UV Stratalinker 1800; Stratagene). The probes were radio-labelled by random priming using [α^{32}P]-dCTP (Hartmann Analytics, Braunschweig, Germany) according to the manufacturer's instructions (ReadyPrime™ labelling kit; Amersham Biosciences). Stringent hybridization and washing conditions were used to minimize cross-hybridization within gene families. The membranes were hybridized overnight at 60°C in the following buffer: 0.25 M sodium phosphate (pH 7.2), 1 mM Na_2EDTA, 6.7% (w/v) SDS, 1% (w/v) BSA. Blots were washed twice in 2x SSC containing 0.1% (w/v) SDS for 10 min at room temperature and once in 2x SSC containing 0.1% (w/v) SDS for 10 min at 60°C. X-ray films were exposed for between 5 and 30 days. As all blots were done using clones of the two *A. halleri* individuals named 3-1 and 5, there can be a minimum of one and a maximum of two alleles per gene copy per lane. When no restriction site was present in the region spanned by the probe, the presence of more than two bands in any one lane was interpreted as an indication for a gene copy number above one. When one restriction site was present in the region spanned by the probe, the presence of more than four bands (two per allele) in a lane was interpreted as an indication for a gene copy number above one. For one 200-bp *Nco*I fragment of *ZIP9* located entirely within a single exon (see Table III), we expected no length polymorphisms between alleles of one gene copy,

based on the sequences of multiple cloned *A. halleri* cDNAs (I.N. Talke, M. Hanikenne, U. Krämer, unpublished data).

Acknowledgements

We thank Anne-Garlonn Desbrosses-Fonrouge for construction of the vector pFL38-GW, and Astrid Schröder for technical support. We thank Susanne Freund, Tomasz Czechowski, Björn Usadel, Toralf Senger, Leonard Krall (Max Planck Institute of Molecular Plant Physiology) and Florian Wagner (Resource Center and Primary Database, Berlin, Germany) for helpful discussions.

Literature Cited

Assunção AGL, Da Costa Martins P, De Folter S, Vooijs R, Schat H, Aarts MGM (2001) Elevated expression of metal transporter genes in three accessions of the metal hyperaccumulator *Thlaspi caerulescens*. Plant Cell Environ **24:** 217-226

Axelsen KB, Palmgren MG (2001) Inventory of the superfamily of P-type ion pumps in *Arabidopsis*. Plant Physiol **126:** 696-706

Baker AJM, Brooks RR (1989) Terrestrial higher plants which hyperaccumulate metallic elements - a review of their distribution, ecology and phytochemistry. Biorecovery **1:** 81-126

Baker AJM, Reeves RD, Hajar ASM (1994) Heavy metal accumulation and tolerance in British populations of the metallophyte *Thlaspi caerulescens* J. & C. Presl (*Brasicaceae*). New Phytol **127:** 61-68

Becher M, Talke IN, Krall L, Krämer U (2004) Cross-species microarray transcript profiling reveals high constitutive expression of metal homeostasis genes in shoots of the zinc hyperaccumulator *Arabidopsis halleri*. Plant J **37:** 251-268

Benjamini Y, Hochberg Y (1995) Controlling false discovery rate: A practical and powerful approach to multiple testing. J R Stat Soc B **57:** 289-300

Bernard C, Roosens N, Czernic P, Lebrun M, Verbruggen N (2004) A novel CPx-ATPase from the cadmium hyperaccumulator *Thlaspi caerulescens*. FEBS Lett **569:** 140-148

Bert V, Bonnin I, Saumitou-Laprade P, de Laguerie P, Petit D (2002) Do *Arabidopsis halleri* from nonmetallicolous populations accumulate zinc and cadmium more effectively than those from metallicolous populations? New Phytol **155:** 47-57

Bert V, Macnair MR, de Laguerie P, Saumitou-Laprade P, Petit D (2000) Zinc tolerance and accumulation in metallicolous and nonmetallicolous populations of *Arabidopsis halleri* (Brassicaceae). New Phytol **146:** 225-233

Bert V, Meerts P, Saumitou-Laprade P, Salis P, Gruber W, Verbruggen N (2003) Genetic basis of Cd tolerance and hyperaccumulation in *Arabidopsis halleri*. Plant Soil **249:** 9-18

Blaudez D, Kohler A, Martin F, Sanders D, Chalot M (2003) Poplar Metal Tolerance Protein 1 (MTP1) Confers Zinc Tolerance and Is an Oligomeric Vacuolar Zinc Transporter with an Essential Leucine Zipper Motif. Plant Cell **15:** 2911-2928

Bonneaud N, Ozier-Kalogeropoulos O, Li GY, Labouesse M, Minvielle-Sebastia L, Lacroute F (1991) A family of low and high copy replicative, integrative and single-stranded *S. cerevisiae*/*E. coli* shuttle vectors. Yeast **7:** 609-615

Clemens S (2001) Molecular mechanisms of plant metal tolerance and homeostasis. Planta **212:** 475-486

Clemens S, Palmgren MG, Krämer U (2002) A long way ahead: Understanding and engineering plant metal accumulation. Trends Plant Sci **7:** 309-315

Conklin DS, McMaster JA, Culbertson MR, Kung C (1992) *COT1*, a gene involved in cobalt accumulation in *Saccharomyces cerevisiae*. Mol Cell Biol **12:** 3678-3688

Curie C, Panaviene Z, Loulergue C, Dellaporta SL, Briat JF, Walker EL (2001) Maize *yellow stripe1* encodes a membrane protein directly involved in Fe(III) uptake. Nature **409:** 346-349

Czechowski T, Bari RP, Stitt M, Scheible WR, Udvardi MK (2004) Real-time RT-PCR profiling of over 1400 Arabidopsis transcription factors: unprecedented sensitivity reveals novel root- and shoot-specific genes. Plant J **38:** 366-379

Dahmani-Muller H, van OF, Gelie B, Balabane M (2000) Strategies of heavy metal uptake by three plant species growing near a metal smelter. Environ Pollut **109:** 231-238

Delhaize E (1996) A metal-accumulator mutant of *Arabidopsis thaliana*. Plant Physiol **111:** 849-855

Delhaize E, Kataoka T, Hebb DM, White RG, Ryan PR (2003) Genes encoding proteins of the cation diffusion facilitator family that confer manganese tolerance. Plant Cell **15:** 1131-1142

Desbrosses-Fonrouge AG, Voigt K, Schröder A, Arrivault S, Thomine S, Krämer U (2005) *Arabidopsis thaliana* MTP1 is a Zn transporter in the vacuolar membrane which mediates Zn detoxification and drives leaf Zn accumulation. FEBS Lett **579:** 4165-4174

Dohmen RJ, Strasser AW, Honer CB, Hollenberg CP (1991) An efficient transformation procedure enabling long-term storage of competent cells of various yeast genera. Yeast **7:** 691-692

Dräger DB, Desbrosses-Fonrouge AG, Krach C, Chardonnens AN, Meyer RC, Saumitou-Laprade P, Krämer U (2004) Two genes encoding *Arabidopsis halleri* MTP1 metal transport proteins co-segregate with zinc tolerance and account for high *MTP1* transcript levels. Plant J **39:** 425-439

Ernst WHO (1974) Schwermetallvegetationen der Erde. Gustav Fischer Verlag, Stuttgart, Germany

Fristedt U, van Der Rest M, Poolman B, Konings WN, Persson BL (1999) Studies of cytochrome c oxidase-driven H(+)-coupled phosphate transport catalyzed by the *Saccharomyces cerevisiae* Pho84 permease in co-reconstituted vesicles. Biochemistry **38:** 16010-16015

Gao M, Li G, McCombie WR, Quiros CF (2005) Comparative analysis of a transposon-rich *Brassica oleracea* BAC clone with its corresponding sequence in *A. thaliana*. Theor Appl Genet **111:** 949-955

Gong Q, Li P, Ma S, Indu Rupassara S, Bohnert HJ (2005) Salinity stress adaptation competence in the extremophile *Thellungiella halophila* in comparison with its relative *Arabidopsis thaliana*. Plant J **44:** 826-839

Green LS, Rogers EE (2004) FRD3 controls iron localization in Arabidopsis. Plant Physiol **136:** 2523-2531

Grotz N, Fox T, Connolly E, Park W, Guerinot ML, Eide D (1998) Identification of a family of zinc transporter genes from Arabidopsis that respond to zinc deficiency. Proc Natl Acad Sci USA **95:** 7220-7224

Hammond JP, Bowen HC, White PJ, Mills V, Pyke KA, Baker AJ, Whiting SN, May ST, Broadley MR (2006) A comparison of the *Thlaspi caerulescens* and *Thlaspi arvense* shoot transcriptomes. New Phytol **170:** 239-260

Houston NL, Fan C, Xiang JQ, Schulze JM, Jung R, Boston RS (2005) Phylogenetic analyses identify 10 classes of the protein disulfide isomerase family in plants, including single-domain protein disulfide isomerase-related proteins. Plant Physiol **137:** 762-778

Hussain D, Haydon MJ, Wang Y, Wong E, Sherson SM, Young J, Camakaris J, Harper JF, Cobbett CS (2004) P-type ATPase heavy metal transporters with roles in essential zinc homeostasis in Arabidopsis. Plant Cell **16:** 1327-1339

Inan G, Zhang Q, Li P, Wang Z, Cao Z, Zhang H, Zhang C, Quist TM, Goodwin SM, Zhu J, Shi H, Damsz B, Charbaji T, Gong Q, Ma S, Fredricksen M, Galbraith DW, Jenks MA, Rhodes D, Hasegawa PM, Bohnert HJ, Joly RJ, Bressan RA, Zhu JK (2004) Salt cress. A halophyte and cryophyte Arabidopsis relative model system and its applicability to molecular genetic analyses of growth and development of extremophiles. Plant Physiol **135:** 1718-1737

Ishizaki K, Shimizu-Ueda Y, Okada S, Yamamoto M, Fujisawa M, Yamato KT, Fukuzawa H, Ohyama K (2002) Multicopy genes uniquely amplified in the Y chromosome-specific repeats of the liverwort *Marchantia polymorpha*. Nucleic Acids Res **30:** 4675-4681

Jensen LT, Ajua-Alemanji M, Culotta VC (2003) The *Saccharomyces cerevisiae* high affinity phosphate transporter encoded by *PHO84* also functions in manganese homeostasis. J Biol Chem **278:** 42036-42040

Kim KN, Fisher DK, Gao M, Guiltinan MJ (1998) Genomic organization and promoter activity of the maize starch branching enzyme I gene. Gene **216:** 233-243

Koch M, Haubold B, Mitchell-Olds T (2001) Molecular systematics of the Brassicaceae: Evidence from coding plastidic *matK* and nuclear *Chs* sequences. Am J Bot **88:** 534-544

Koch MA, Haubold B, Mitchell-Olds T (2000) Comparative evolutionary analysis of chalcone synthase and alcohol dehydrogenase loci in *Arabidopsis*, *Arabis*, and related genera (*Brassicaceae*). Mol Biol Evol **17:** 1483-1498

Krämer U, Clemens S (2005) Functions and homeostasis of zinc, copper, and nickel in plants. *In* M Tamás, E Martinoia, eds, Molecular Biology of Metal Homeostasis and Detoxification, Top Curr Genet, Vol 14, pp 216-271

Krämer U, Cotter-Howells JD, Charnock JM, Baker AJM, Smith JAC (1996) Free histidine as a metal chelator in plants that accumulate nickel. Nature **379:** 635-638

Kubota H, Takenaka C (2003) Arabis gemmifera is a hyperaccumulator of Cd and Zn. Int J Phytoremediation **5:** 197-201

Küpper H, Lombi E, Zhao FJ, McGrath SP (2000) Cellular compartmentation of cadmium and zinc in relation to other elements in the hyperaccumulator *Arabidopsis halleri*. Planta **212:** 75-84

Lahner B, Gong J, Mahmoudian M, Smith EL, Abid KB, Rogers EE, Guerinot ML, Harper JF, Ward JM, McIntyre L, Schroeder JI, Salt DE (2003) Genomic scale profiling of nutrient and trace elements in *Arabidopsis thaliana*. Nat Biotechnol **21:** 1215-1221

Lanquar V, Lelievre F, Bolte S, Hames C, Alcon C, Neumann D, Vansuyt G, Curie C, Schroder A, Kramer U, Barbier-Brygoo H, Thomine S (2005) Mobilization of vacuolar iron by AtNRAMP3 and AtNRAMP4 is essential for seed germination on low iron. Embo J **24:** 4041-4051

Lasat MM, Pence NS, Garvin DF, Ebbs SD, Kochian LV (2000) Molecular physiology of zinc transport in the Zn hyperaccumulator *Thlaspi caerulescens*. J Exp Bot **51:** 71-79

Macnair MR, Bert V, Huitson SB, Saumitou-Laprade P, Petit D (1999) Zinc tolerance and hyperaccumulation are genetically independent characters. Proc R Soc Lond B Biol Sci **266:** 2175-2179

Marquardt J, Wans S, Rhiel E, Randolf A, Krumbein WE (2000) Intron-exon structure and gene copy number of a gene encoding for a membrane-intrinsic light-harvesting polypeptide of the red alga *Galdieria sulphuraria*. Gene **255:** 257-265

Mäser P, Thomine S, Schroeder JI, Ward JM, Hirschi K, Sze H, Talke IN, Amtmann A, Maathuis FJ, Sanders D, Harper JF, Tchieu J, Gribskov M, Persans MW, Salt DE, Kim SA, Guerinot ML (2001) Phylogenetic relationships within cation transporter families of Arabidopsis. Plant Physiol **126:** 1646-1667

McKie AT, Barlow DJ (2004) The SLC40 basolateral iron transporter family (IREG1/ferroportin/MTP1). Pflugers Arch **447:** 801-806

Mills RF, Francini A, Ferreira da Rocha PS, Baccarini PJ, Aylett M, Krijger GC, Williams LE (2005) The plant P_{1B}-type ATPase AtHMA4 transports Zn and Cd and plays a role in detoxification of transition metals supplied at elevated levels. FEBS Lett **579:** 783-791

Mirouze M, Sels J, Richard O, Czernic P, Loubet S, Jacquier A, François IEJA, Cammue BPA, Lebrun M, Berthomieu P, Marquès L (2006) A putative novel role for plant defensins: a defensin from the zinc hyperaccumulating plant, *Arabidopsis halleri*, confers zinc tolerance. Plant J **in press**

Narindrasorasak S, Yao P, Sarkar B (2003) Protein disulfide isomerase, a multifunctional protein chaperone, shows copper-binding activity. Biochem Biophys Res Commun **311:** 405-414

Papoyan A, Kochian LV (2004) Identification of *Thlaspi caerulescens* genes that may be involved in heavy metal hyperaccumulation and tolerance. Characterization of a novel heavy metal transporting ATPase. Plant Physiol **136:** 3814-3823

Peleman J, Saito K, Cottyn B, Engler G, Seurinck J, Van Montagu M, Inze D (1989) Structure and expression analyses of the S-adenosylmethionine synthetase gene family in *Arabidopsis thaliana*. Gene **84:** 359-369

Pence NS, Larsen PB, Ebbs SD, Letham DL, Lasat MM, Garvin DF, Eide D, Kochian LV (2000) The molecular physiology of heavy metal transport in the Zn/Cd hyperaccumulator *Thlaspi caerulescens*. Proc Natl Acad Sci USA **97:** 4956-4960

Persans MW, Nieman K, Salt DE (2001) Functional activity and role of cation-efflux family members in Ni hyperaccumulation in *Thlaspi goesingense*. Proc Natl Acad Sci USA **98:** 9995-10000

Petit JM, Briat JF, Lobreaux S (2001) Structure and differential expression of the four members of the *Arabidopsis thaliana* ferritin gene family. Biochem J **359:** 575-582

Pich A, Scholz G (1996) Translocation of copper and other micronutrient in tomato plants (*Lycopersicon esculentum* Mill.): nicotianamine-stimulated copper transport in the xylem. J Exp Bot **47:** 41-47

Pich A, Scholz G, Stephan UW (1994) Iron-dependent changes of heavy metals, nicotianamine, and citrate in different plant organs and in the xylem exudate of two tomato genotypes. Nicotianamine as possible copper translocator. Plant Soil **165:** 189-196

Ramakers C, Ruijter JM, Deprez RH, Moorman AF (2003) Assumption-free analysis of quantitative real-time polymerase chain reaction (PCR) data. Neurosci Lett **339:** 62-66

Reeves RD, Baker AJM (2000) Metal-accumulating plants. *In* I Raskin, BD Ensley, eds, Phytoremediation of toxic metals: Using plants to clean up the environment. John Wiley & Sons, Inc., Hoboken, NJ, pp 193-230

Rensing C, Mitra B, Rosen BP (1997) Insertional inactivation of *dsbA* produces sensitivity to cadmium and zinc in *Escherichia coli*. J Bacteriol **179:** 2769-2771

Rogers EE, Guerinot ML (2002) FRD3, a member of the multidrug and toxin efflux family, controls iron deficiency responses in *Arabidopsis*. Plant Cell **14:** 1787-1799

Roosens NH, Bernard C, Leplae R, Verbruggen N (2004) Evidence for copper homeostasis function of metallothionein (MT3) in the hyperaccumulator *Thlaspi caerulescens*. FEBS Lett **577:** 9-16

Salt DE, Krämer U (2000) Mechanisms of metal hyperaccumulation in plants. *In* I Raskin, Ensley, B.D., ed, Phytoremediation of toxic metals: Using plants to clean up the environment. John Wiley & Sons, Inc., Hoboken, NJ, pp 231-246

Sambrook J, Russel DW (2001) Molecular Cloning - A Laboratory Manual. Cold Spring Harbor Laboratory Press, Cold Spring Harbor, New York

Sarret G, Saumitou-Laprade P, Bert V, Proux O, Hazemann JL, Traverse A, Marcus MA, Manceau A (2002) Forms of zinc accumulated in the hyperaccumulator *Arabidopsis halleri*. Plant Physiol **130:** 1815-1826

Sentenac H, Bonneaud N, Minet M, Lacroute F, Salmon JM, Gaymard F, Grignon C (1992) Cloning and expression in yeast of a plant potassium ion transport system. Science **256:** 663-665

Shikanai T, Muller-Moule P, Munekage Y, Niyogi KK, Pilon M (2003) PAA1, a P-type ATPase of *Arabidopsis*, functions in copper transport in chloroplasts. Plant Cell **15:** 1333-1346

Shin H, Shin HS, Dewbre GR, Harrison MJ (2004) Phosphate transport in Arabidopsis: Pht1;1 and Pht1;4 play a major role in phosphate acquisition from both low- and high-phosphate environments. Plant J **39:** 629-642

Small RL, Wendel JF (2000) Copy number lability and evolutionary dynamics of the *Adh* gene family in diploid and tetraploid cotton (Gossypium). Genetics **155:** 1913-1926

Taji T, Seki M, Satou M, Sakurai T, Kobayashi M, Ishiyama K, Narusaka Y, Narusaka M, Zhu JK, Shinozaki K (2004) Comparative genomics in salt tolerance between Arabidopsis and Arabidopsis-related halophyte salt cress using Arabidopsis microarray. Plant Physiol **135:** 1697-1709

Thomine S, Lelievre F, Debarbieux E, Schroeder JI, Barbier-Brygoo H (2003) AtNRAMP3, a multispecific vacuolar metal transporter involved in plant responses to iron deficiency. Plant J **34:** 685-695

Thomine S, Wang R, Ward JM, Crawford NM, Schroeder JI (2000) Cadmium and iron transport by members of a plant metal transporter family in Arabidopsis with homology to *Nramp* genes. Proc Natl Acad Sci USA **97:** 4991-4996

Usadel B, Nagel A, Thimm O, Redestig H, Bläsing OE, Palacios-Rojas N, Selbig J, Hannemann J, Piques MC, Steinhauser D, Scheible WR, Gibon Y, Morcuende R, Weicht D, Meyer S, Stitt M (2005) Extension of the visualization tool MapMan to allow statistical analysis of arrays, display of corresponding genes, and comparison with known responses. Plant Physiol **138:** 1195-1204

Verret F, Gravot A, Auroy P, Leonhardt N, David P, Nussaume L, Vavasseur A, Richaud P (2004) Overexpression of AtHMA4 enhances root-to-shoot translocation of zinc and cadmium and plant metal tolerance. FEBS Lett **576:** 306-312

von Wiren N, Klair S, Bansal S, Briat JF, Khodr H, Shioiri T, Leigh RA, Hider RC (1999) Nicotianamine chelates both Fe(III) and Fe(II). Implications for metal transport in plants. Plant Physiol **119:** 1107-1114

Weber M, Harada E, Vess C, von Roepenack-Lahaye E, Clemens S (2004) Comparative microarray analysis of *Arabidopsis thaliana* and *Arabidopsis halleri* roots identifies nicotianamine synthase, a ZIP transporter and other genes as potential metal hyperaccumulation factors. Plant J **37:** 269-281

Wintz H, Fox T, Wu YY, Feng V, Chen W, Chang HS, Zhu T, Vulpe C (2003) Expression profiles of *Arabidopsis thaliana* in mineral deficiencies reveal novel transporters involved in metal homeostasis. J Biol Chem **278:** 47644-47653

Yogeeswaran K, Frary A, York TL, Amenta A, Lesser AH, Nasrallah JB, Tanksley SD, Nasrallah ME (2005) Comparative genome analyses of Arabidopsis spp.: inferring chromosomal rearrangement events in the evolutionary history of *A. thaliana*. Genome Res **15:** 505-515

Figure legends

Figure 1. Long-term Zn accumulation in *A. halleri* and *A. thaliana* roots and shoots. Hydroponically grown 4.5-week old plants were supplied with different Zn concentrations in the culture medium for 3 weeks before harvest. The Zn concentrations in (A) root and (B) shoot tissues

were determined by inductively coupled plasma optical emission spectroscopy (ICP-OES); open circles: *A. thaliana*; filled circles: *A. halleri*. (C) illustrates the ratio of Zn concentrations in shoot *vs*. root tissues. Note that at 10 µM $ZnSO_4$, the Zn concentration in *A. thaliana* roots exceeds that of *A. halleri* roots by more than 30-fold. In preliminary experiments, exposure of hydroponically grown *A. thaliana* to 30 µM $ZnSO_4$ for a period of 3 weeks led to the onset of mild toxicity symptoms; therefore this Zn condition was excluded. Data are from one experiment representative of two independent experiments. Values represent mean ± standard error, calculated from $n = 3$ culture vessels per Zn condition. For C, data were $\log_2$ transformed. Data were plotted with OriginPro 7 SR4 (v 7.0552; OriginLab Corporation, Northampton, MA, USA) and logarithmic fits to the data were performed for A and B, a cubic B-spline connection was used for the smooth curves in C.

Figure 2. Expression analysis of known Zn-regulated marker genes. Real-time RT-PCR analysis of expression of *ZIP4*, *ZIP9* and *NAS2* genes in roots (top panel) and shoots (bottom panel) of hydroponically grown *A. halleri* (black bars) and *A. thaliana* (light grey bars). Two different basal Zn conditions upon which additional Zn was supplied were assessed: "Short Zn oversupply" denotes a short-term high Zn supply to plants pre-cultivated at control Zn concentrations; for *A. thaliana*, 30 µM Zn, and for *A. halleri*, 300 µM Zn were added to the culture medium for 2 and 8 h before harvest. "Zn deficiency / resupply" denotes a supply of 5 µM Zn to Zn-deficient plants for 2, 8 and 24 h before harvest. Note that substantial changes in root transcript levels occur as soon as 2 h after the change of Zn concentration in the culture medium whereas shoot transcript levels reflect the change in external Zn supply only at a later time point. Data shown are transcript levels relative to *EF1*α from one experiment representative of two independent biological experiments. Tissues from at least three culture vessels containing three plants each were pooled for each condition. Genes were concluded to be not expressed (n. e.) when C_T values were above a threshold of 35 and reaction efficiencies with the respective cDNA were more than 5% below the mean reaction efficiency for the respective primer pair (see also Materials and Methods).

Figure 3. The relation between ATH1 microarray signals of GeneChips hybridized with cRNA from *A. halleri* and from *A. thaliana* grown under control Zn conditions. For each of the 22,810 probe sets on the ATH1 array, the mean signal derived from the two replicate arrays of (A) roots and (B) shoots of *A. halleri* was plotted on the *y* axis and the respective mean signal of *A. thaliana* was plotted on the *x* axis. Signal values represent mean signal intensities calculated from MAS 5.0-scaled raw signals of replicate arrays, without further normalization. Symbols and colors reflect the data filtering which was applied in order to identify candidate genes more highly expressed in *A. halleri* compared to *A. thaliana* and involved in metal ion homeostasis or related processes. Grey

diamonds represent all probe sets that did not pass any filter. Yellow squares represent probe sets that exhibited a fourfold higher signal intensity in *A. halleri* than in *A. thaliana* and passed the value filter (for details see Materials and Methods). Blue triangles represent probe sets that, in addition, passed a first annotation filter (I) of genes annotated as metal ion (Zn, Fe, Cu, Mn) binding, membrane and transport-associated, oxidative stress protection-associated, pathogen response-related and RNA metabolism-associated (Supplemental Table XI). Red circles represent probe sets that passed a further annotation filter (II) which included only genes with a predicted function in metal ion homeostasis. Candidate genes that passed the value filter and either annotation filter and which were chosen for further analysis by real-time RT-PCR are represented by green triangles (passed annotation filter I) or circles (passed annotation filter II) with a black outline (for details see Table I).

Figure 4. Functional analysis of *AtHMA4* and *AhHMA4* cDNAs in *S. cerevisiae* mutant strains.
(A) Expression of Arabidopsis *HMA4* cDNAs in the Zn-hypersensitive *zrc1 cot1* double mutant and (B) in the Cd-hypersensitive *ycf1* mutant. (A, B) Wild-type cells were transformed with pFL38H-GW (ev), and mutant cells were transformed with pFL38H-GW (ev) and with wild-type and mutated (D401A) cDNAs of both *AtHMA4* and *AhHMA4* in pFL38H-GW. The phosphorylation of the aspartate residue (here D401) of the conserved phosphorylation motif is an indispensable step of the reaction cycle in all P-type ATPases. Serial dilutions of transformants were spotted on LSP plates containing the indicated concentrations of $ZnSO_4$ (A) or $CdSO_4$ (B). The 10^0 dilution corresponds to an OD_{600} of 0.5. Plates were incubated at 30°C for 4 days.

Figure 5. Genomic DNA gel blot for (A) *ZIP9*, (B) *HMA4*, (C) *FRD3* and (D) *MTP8* in *A. thaliana* and in *A. halleri*. Blots were performed using genomic DNA extracted from *A. thaliana* (Col accession) and from two *A. halleri* individuals (Lan 3-1 and Lan 5 of the accession Langelsheim). (A) to (D) Five µg of genomic DNA were digested with *Eco*RI, *Hind*III or *Nco*I, resolved on a 0.9% (w/v) agarose gel, blotted and hybridized with radio-labelled *A. halleri*-derived cDNA probes. (A) An *Eco*RI restriction site is present in the region spanned by the *ZIP9* probe in *A. thaliana* only, an *Hind*III restriction site is present in the intron spanned by the probe in *A. halleri* only, and an *Nco*I restriction site is present in an exon spanned by the probe in both species. (B) An *Hind*III restriction site is present in one of the introns spanned by the *HMA4* probe in *A. halleri*. (C) An *Hind*III restriction site is present in the region spanned by the *FRD3* probe in both species. (D) After restriction with *Nco*I, a predicted 20.9 kBp fragment in *A. thaliana* was not detected by the *MTP8*

probe, probably because of the large size of this fragment (see also Table III). Note that for clarity, lanes were rearranged in the *ZIP9* blot.

Figure 6. Transcriptional responses of selected candidate genes to Zn and other ions. Transcript levels relative to *EF1α* were assessed in (A) roots and (B) shoots of hydroponically grown plants subjected to short-term treatment with high Zn, long-term Zn deficiency or short-term treatment with Cd, Cu or Na (see Materials and Methods for details). Relative transcript levels (RTL) within a treatment were normalized to the RTL of the control treatment in the respective experiment ("relative transcript level normalized to control"). To determine transcriptional responses for each treatment and each gene, the mean relative transcript level normalized to control was calculated from the respective values from two independent biological experiments. Bold letters indicate genes that exhibit higher transcript levels in *A. halleri* compared to *A. thaliana* after cultivation in the presence of control Zn concentrations. Note that some genes were not expressed in some conditions, see Figures 2 and 7 for details.

Figure 7. Zn-dependent transcriptional regulation of selected candidate genes. Real-time RT-PCR analysis of expression of *HMA4*, *ZIP3* and *IRT3* genes in roots (top panel) and shoots (bottom panel) of hydroponically grown *A. halleri* (black bars) and *A. thaliana* (light grey bars). Two different basal Zn conditions upon which additional Zn was supplied were assessed: "Short Zn oversupply" and "Zn deficiency / resupply". For a detailed description, see Figure 2 and Materials and Methods. Data shown are transcript levels relative to *EF1α* from one experiment representative of two independent biological experiments. Tissues from at least three culture vessels with three plants each were pooled for each condition. Genes were concluded to be not expressed (n. e.) when C_T values were above a threshold of 35 and reaction efficiencies with the respective cDNA were more than 5% below the mean reaction efficiency for the respective primer pair. Note that *ZIP3* was "not expressed" in shoots only for the condition "*A. thaliana*, 8 h 30 µM Zn supply". At all other conditions, *ZIP3* transcripts were detectable but relative transcript levels (RTL) were very low (*A. h.*: 4.3 [control], 3.5 [2 h] and 2.6 [8 h]; *A. t.*: 1.7 [control], 1.7 [2 h] and 3.9 [control Zn deficiency]), and therefore do not appear as visible bars in the diagram.

Supplemental data figure legends

Supplemental Figure 1. Genomic DNA gel blot for (A) *ZIP3*, (B) *ZIP4*, (C) *ZIP10*, (D) *IRT3*, (E) *ZIP6*, (F) *PHT1;4*, (G) *PDI1* and (H) *PDI2* genes in *A. thaliana* and in *A. halleri*. Blots were performed using genomic DNA extracted from *A. thaliana* (Col accession) and from two *A. halleri*

individuals (Lan 3-1 and Lan 5 of the accession Langelsheim). (A) to (H) Five µg of genomic DNA were digested with *Eco*RI, *Hind*III or *Nco*I, resolved on a 0.9% (w/v) agarose gel, blotted and hybridized with radio-labelled *A. halleri*-derived cDNA probes. The size of the detected fragments, the presence of *Eco*RI, *Hind*III or *Nco*I restriction sites in the probe region, and an estimate of the gene copy number in *A. halleri* are given in Table III. White asterisks indicate bands arising from cross-hybridization of the *AhZIP3* probe with the *AtZIP5* genomic sequence (A), *AhIRT3* and *AhZIP4* probes with *AtZIP4* and *AtIRT3* genomic sequences (B, D) and *AhPDI1* and *AhPDI2* probes with *AtPDI2* and *AtPDI1* genomic sequences (F, G), respectively.

Table I. Summary of microarray data for *A. halleri* root and shoot candidate genes

ATH1 probe set identifiers and the corresponding *A. thaliana* locus identifiers are given for candidate genes more highly expressed in *A. halleri* than in *A. thaliana* under control conditions (genes that passed the value filter as described in Materials and Methods). In addition, genes were included that showed an at least two-fold upregulation or downregulation upon short-term Zn supply in *A. halleri*. Raw signal denotes mean signal value calculated from signal values exported from MAS 5.0 using GeneSpring. Microarray data for short-term Zn supply and Zn deficiency are given where the regulation compared to controls was at least two-fold. One sample Student's *t*-tests were performed in GeneSpring on ratios from cross-species and fold changes from within-species comparisons, *P* values are indicated as follows: * = $P < 0.05$; ** = $P < 0.01$; *** = $P < 0.001$.

ATH1 probe set identifier	AGI locus identifier	Gene name	*A. halleri* raw signal	*A. h.* / *A. t.* signal ratio	*A. halleri* fold change - Zn(II)	*A. halleri* fold change + Zn(II), root: 2 h shoot: 8 h	*A. thaliana* fold change + Zn(II), root: 2 h shoot: 8h	Annotation
Root candidates								
Cytoplasmic metal influx								
262546_at	At1g31260	*ZIP10* [b]	141	111 **	3.74			ZIP family of metal transporters
253413_at	At4g33020	*ZIP9*	617	36.2 ***				ZIP family of metal transporters
260462_at	At1g10970	*ZIP4*	722	24.6 ***	2.29	0.31		ZIP family of metal transporters
259723_at	At1g60960	*IRT3* [b]	738	4.47 *	2.79	0.28	0.37 *	ZIP family of metal transporters
257715_at	At3g12750	*ZIP1*	194	4.08 *	2.05			ZIP family of metal transporters
266336_at	At2g32270	*ZIP3* [b]	849	1.71 *		0.37	0.30 *	ZIP family of metal transporters
Root-to-shoot metal transport								
258646_at	At3g08040	*FRD3* [b]	2890	44.6 ***				MATE family transporter
Other membrane transport								
266184_s_at	At2g38940	*PHT1;4* [b]	822	19.1 **				Phosphate:H^+ symporter family, *Sc*Pho84-like
253658_at	At4g30120	*HMA3*	457	9.14 *				P_{1B} CPX metal ATPase family
267266_at	At2g23150	*NRAMP3*	685	6.61 ***				Natural resistance associated macrophage protein family
249255_at	At5g41610	*CHX18* [b]	34.1	6.52 *				Cation/H^+ exchanger of unknown specificity, CPA2 family
266718_at	At2g46800	*MTP1*	1561	6.40 ***				Cation diffusion facilitator family
267029_at	At2g38460	*IREG2* [b]	248	4.49 ***				similar to human iron-regulated Fe-transporter
Nicotianamine/Thiol biosynthesis pathways								
248048_at	At5g56080	*NAS2*	2765	48.4 ***				Nicotianamine synthase
259632_at	At1g56430	*NAS4* [a]	70.1	13.7	2.42			Nicotianamine synthase
264261_at	At1g09240	*NAS3*	106	5.22 **	3.81 *			Nicotianamine synthase
263838_at	At2g36880	*SAMS3* [b]	5353	4.31 *				S-adenosylmethionine synthetase
250832_at	At5g04950	*NAS1* [a]	90.1	0.81				Nicotianamine synthase
Other metal handling								
257365_x_at	At2g26020	*PDF1.2b*	57.15	37.2 *				Plant defensin, antifungal protein AFP5 [d]
Shoot candidates								
Cytoplasmic metal influx								
267304_at	At2g30080	*ZIP6*	288	7.34 ***				ZIP family of metal transporters
260462_at	At1g10970	*ZIP4*	256	4.04 *	12.70 **			ZIP family of metal transporters
Root-to-shoot metal transport								
267488_at	At2g19110	*HMA4* [b]	113	52.5 **				P_{1B} CPX metal ATPase family
Other membrane transport								
253658_at	At4g30120	*HMA3*	796	358 **				P_{1B} CPX metal ATPase family
251620_at	At3g58060	*MTP8* [b]	108	65.0 **				Cation diffusion facilitator family
266718_at	At2g46800	*MTP1*	4862	27.9 ***				Cation diffusion facilitator family
246276_at	At4g37270	*HMA1*	416	12.6 **				P_{1B} CPX metal ATPase family
267266_at	At2g23150	*NRAMP3*	309	7.30 ***				Natural resistance associated macrophage protein family
266963_at	At2g39450	*MTP11* [b]	465	4.74 ***				Cation diffusion facilitator family
253339_at	At4g33520	*HMA6* [b]	148	4.58 **				P_{1B} CPX metal ATPase family; *PAA1*
257789_at	At3g27020	*YSL6* [b]	256	4.42 *			2.54	Yellow-stripe-like transporter family
Nicotianamine/Thiol biosynthesis pathways								
256930_at	At3g22460	*OASA2* [c]	188	10.6 ***	2.43			O-acetylserine thiol lyase
260913_at	At1g02500	*SAMS1* [b]	988	10.4 **			3.68	S-adenosylmethionine synthetase
255552_at	At4g01850	*SAMS2* [b]	1765	8.54 ***			2.10	S-adenosylmethionine synthetase
264261_at	At1g09240	*NAS3*	316	7.89 **	5.01 *			Nicotianamine synthase
263838_at	At2g36880	*SAMS3* [b]	2392	5.31 **			2.04	S-adenosylmethionine synthetase
Other metal handling								
256416_at	At3g11050	*FER2* [b]	83.1	11.0 *				Ferritin, Fe(III) binding
257365_x_at	At2g26020	*PDF1.2b*	5023	7.95 *				Plant defensin, antifungal protein AFP5 [d]
251109_at	At5g01600	*FER1* [b]	6509	5.13 **				Ferritin, Fe(III) binding
Stress protection								
262504_at	At1g21750	*PDI1* [b]	2538	39.5 **			3.76	Protein disulfide isomerase
259757_at	At1g77510	*PDI2* [c]	742	17.5 **			2.65	Protein disulfide isomerase

[a] The microarray data for 259632_at, *NAS4*, and 250832_at, *NAS1*, in roots are given for comparison.
[b] Newly identified candidate gene. [c] Identified as false positive by real-time RT-PCR (Table II). [d] Mirouze et al., 2006.

Table II. Summary of real-time RT-PCR data for selected candidate genes at control Zn concentrations

Transcript levels relative to *EF1α* of selected candidate genes as determined by real-time RT-PCR are given for shoot and root tissues from plants grown under control conditions. Values are mean and standard error of between three and five independent experiments for *A. halleri* and *A. thaliana*. The statistical significances of the differences between *A. halleri* and *A. thaliana* expression levels was assessed with a student's *t*-test (two-sample assuming unequal variances), *P* values are indicated as follows: * = $P < 0.05$; ** = $P < 0.01$; *** = $P < 0.001$. In real-time RT-PCR experiments, genes were determined as not expressed (n. e.) when C_T values were above a threshold of 35 and reaction efficiencies with the respective cDNA were more than 5% below the mean reaction efficiency for the respective primer pair; n.d. = not determined.The normalized –fold difference between *A. halleri* and *A. thaliana* from ATH1 microarray data is given for comparison (see Table 1 for further details). Flags denote "calls" as given by MAS5: P = present; M = marginal; A = absent. *NAS1* and *NAS4* were included for comparison with the other members of the *NAS* family.

	Root							**Shoot**							**Tissue with higher expression in *A. halleri* compared to *A. thaliana***	
	Real-time RT-PCR				**Microarray**			**Real-time RT-PCR**				**Microarray**				
Gene name	*A. halleri* transcript level	*P* value	*A. thaliana* transcript level	*A. h. / A. t.* transcript ratio	*A. h. / A. t.* signal ratio	*A. h.* flag	*A. t.* flag	*A. halleri* transcript level	*P* value	*A. thaliana* transcript level	*A. h. / A. t.* transcript ratio	*A. h. / A. t.* signal ratio	*A. h.* flag	*A. t.* flag	Real-time RT-PCR	Microarray
Cytoplasmic metal influx																
ZIP3	498 ± 46.0	**	108 ± 46.1	4.62	1.71 *	P	P	10.2 ± 2.62	*	1.29 ± 0.43	7.89	2.37	A	A	root, shoot	
ZIP4	155 ± 19.6	***	13.1 ± 1.74	11.9	24.6 ***	P	A	52.6 ± 7.96		92.1 ± 44.3	0.57	4.04 *	P	P	root	root, shoot
ZIP9	654 ± 189	*	50.0 ± 4.61	13.1	36.2 ***	P	P,A	n. e.		n. e.	n. d.	6.32	A	A	root	root
ZIP10	17.9 ± 4.98	*	2.89 ± 0.71	6.18	111 **	P,M	A	n. e.		n. e.	n. d.	3.24	A	A	root	root
IRT3	191 ± 20.5	***	40.9 ± 14.6	4.68	4.47 *	P	P	85.0 ± 4.70		63.8 ± 38.9	1.33	1.70 *	P	P	root	root
ZIP6	122 ± 27.9	*	26.3 ± 4.78	4.64	2.16 *	P	P	183 ± 33.5	**	18.2 ± 5.35	10.1	7.34 ***	P	M,A	root, shoot	shoot
Root-to-shoot metal transport																
HMA4	2092 ± 401	**	327 ± 29.2	6.39	0.71	P	P	1141 ± 332	*	37.9 ± 31.4	30.1	52.5 **	P	A	root, shoot	shoot
FRD3	292 ± 87.8	*	18.8 ± 4.95	15.5	44.6 ***	P	P	46.5 ± 13.3	*	7.45 ± 3.05	6.23	37.1 *	P	A	root, shoot	root
Other membrane transport																
MTP8	10.6 ± 3.53	*	1.39 ± 0.53	7.65	15.9 *	A	A	32.4 ± 7.84	*	2.86 ± 1.45	11.3	65.0 **	P,A	A	root, shoot	shoot
PHT1;4	77.6 ± 15.9	*	18.7 ± 1.43	4.15	19.1 **	P	P	108 ± 10.2	***	20.2 ± 10.3	5.33	446 *	P	A	root, shoot	root
Nicotianamine/Thiol biosynthesis pathways																
NAS1	52.0 ± 10.4		49.5 ± 24.9	1.05	0.81	P	P	37.4 ± 9.27		79.3 ± 26.7	0.47	0.54	P,M	P		
NAS2	437 ± 113	*	27.5 ± 14.9	15.9	48.4 ***	P	P	n. e.		n. e.	n. d.	3.14	P,A	A	root	root
NAS3	13.9 ± 2.55	**	0.20 ± 0.05	71.4	5.22 **	P	A	44.7 ± 5.06	*	15.8 ± 6.43	2.82	7.89 **	P	P	root, shoot	root, shoot
NAS4	12.3 ± 1.54		6.93 ± 2.12	1.78	13.7	P,M	A	34.5 ± 10.4	*	125 ± 34.6	0.28	0.36 *	P	P		
OASA2	22.7 ± 5.28		83.5 ± 27.1	0.27	3.25 *	P	P	13.3 ± 2.08		64.7 ± 30.8	0.21	10.6 ***	P	P		shoot
SAMS2	881 ± 140	**	158 ± 36.4	5.59	2.60 *	P	P	422 ± 65.4	**	70.6 ± 24.6	5.97	8.54 ***	P	P	root, shoot	shoot
Stress protection																
PDI1	362 ± 56.7	*	173 ± 42.9	2.10	3.50 **	P	P	355 ± 63.3	*	91.3 ± 47.1	3.89	39.5 **	P	P	root, shoot	shoot
PDI2	118 ± 20.4		125 ± 48.8	0.94	3.08 *	P	P	129 ± 16.9		127 ± 49.3	1.01	17.5 **	P	P		shoot

Table III. Gene copy number estimated by genomic DNA gel blot for selected candidate genes in *A. halleri*.

Five µg of genomic DNA isolated from *A. thaliana* (Col-0 accession) and from two *A. halleri* individuals (Lan 3-1 and Lan 5 of the Langelsheim accession) were digested with *Eco*RI, *Hind*III or *Nco*I, resolved on a 0.9% (w/v) agarose gel, blotted and hybridized with radio-labelled *A. halleri*-derived cDNA probes. The size of the detected DNA fragments is given in kBp (detectable fragments were in the range of 0.2 and 14 kBp). Note that in *A. halleri*, there are a maximum of two alleles per gene copy. Blots for the 4 underlined genes are presented in Figure 5, and other blots are shown in Supplemental Figure 1.

Gene	Copy No. in *A. h.*	*A. halleri* Lan 3.1			*A. halleri* Lan 5			*A. thaliana* Col-0		
		*Eco*RI	*Hind*III	*Nco*I	*Eco*RI	*Hind*III	*Nco*I	*Eco*RI	*Hind*III	*Nco*I
ZIP3	**> 1**	3.5 1.2	6.5 5.8 1.5	>10	3.5 1.2	6.5 5.8 1.5	>10	3.6 (3.8)[d]	7.4 (5.4)[d]	15.2 (7.2)[d] (1.7)[d]
ZIP4	**~ 1**	4.2 0.8	2.2 1.5	0.6	4.2 0.8	2.2 1.5	0.6	0.8 (6.3)[e]	7.0 (5.5)[e] (2.0)[e,i]	2.0 (4.5)[e]
ZIP9	**> 1**	5.5	2.5[c] 1.7 0.7	4[a] 2 0.2	5.5 3.5	2.5[c] 1.7 0.7	4[a] 2.2 2 0.2	4.2[c] 0.5	4.4	4.0[a] 0.2
ZIP10	**~ 1**	3.2	2.8	-[i]	3.2 3	3 2.8	4	14.4[i]	2.9	28.6[i]
IRT3	**~ 1**	1.5 0.9	2.2[a] 2 1.5 1	9.5 0.8	1.5 0.9	2.2[a] 2 1.5	9.5 0.8	6.3 (0.8)[e]	(7.0)[e] 5.5[b] 2.0 0.06[e]	4.5 (2.0)[e]
ZIP6	**> 1**	10 5 2.5 2	5.8 4	>10 9	5 2.5	6 3.8 2.2	>10 9	2.7[i]	8.4	11.7
HMA4	**> 1**	10 8	6[c] 4.5 1.7 1.2 0.6	9 7.5 3.8	10 8	6[c] 4.5 4 1.2 0.6	9 7.5	15.7	2.8[c] 0.6	7.3 (4.1)[f]
FRD3	**~ 1**	>10 8	3.5[a,i]	10	>10	3.5[a,i]	10	1.5	3.5[a] 1.0	14.9
MTP8	**~ 1**	5	1.1	-[i]	5	1.1	-[i]	5.7	1.1	20.9[i]
PHT1;4	**~ 1**	1	-[j]	4	1	-[i]	4	10.0 (2.0)[g]	6.0 (2.5)[g]	4.1 (5.9)[g]
PDI1	**~ 1**	1.5	3.3 1 0.7 0.6	2.2	2.4	3.3 1 0.7 0.6	2.2	(3.4)[h] 2.4 (1.5)[j]	3.0[a,c] (2.4)[h] (1.0)[h] 0.65 0.56	2.2 (2.0)[h]
PDI2	**~ 1**	1.5	3.3 1 0.7 0.6	2.2	2.4	3.3 1 0.7 0.6	2.2	3.4 (2.4)[h] (1.5)[j]	(3.0)[h] 2.4[c] 1.0 (0.65)[h] (0.56)[h]	2.8[a] 2.0 (2.2)[h]

[a] Enzyme cuts once in the probe. [b] Enzyme cuts twice in the probe. [c] Enzyme cuts once in one of the intron spanned by the cDNA probe. [d] Cross-hybridisation of *AhZIP3* probe with *AtZIP5* genomic sequence. [e] Cross-hybridisation of *AhIRT3* and *AhZIP4* probes with *AtZIP4* and *AtIRT3* genomic sequences, respectively. [f] Cross-hybridisation of *AhHMA4* probe with *AtHMA2* genomic sequence. [g] Cross-hybridisation of *AhPht1;4* probe with *At3g54700* genomic sequence. [h] Cross-hybridisation of *AhPDI1* and *AhPDI2* probes with *AtPDI2* and *AtPDI1* genomic sequences, respectively. Note that it is likely that cross-hybridization also occurs of *AhPDI1* and *AhPDI2* probes with *AhPDI2* and *AhPDI1* genomic sequences. [i] Not detected, predicted fragment given for *A. thaliana*. [j] Additional band, identity not known.

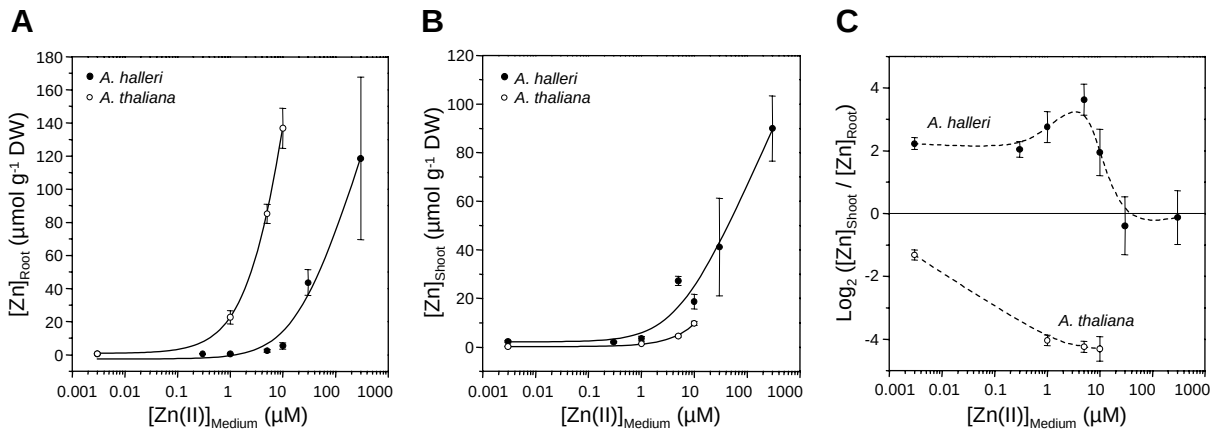

Figure 1 – Talke *et al.*

Root transcript levels

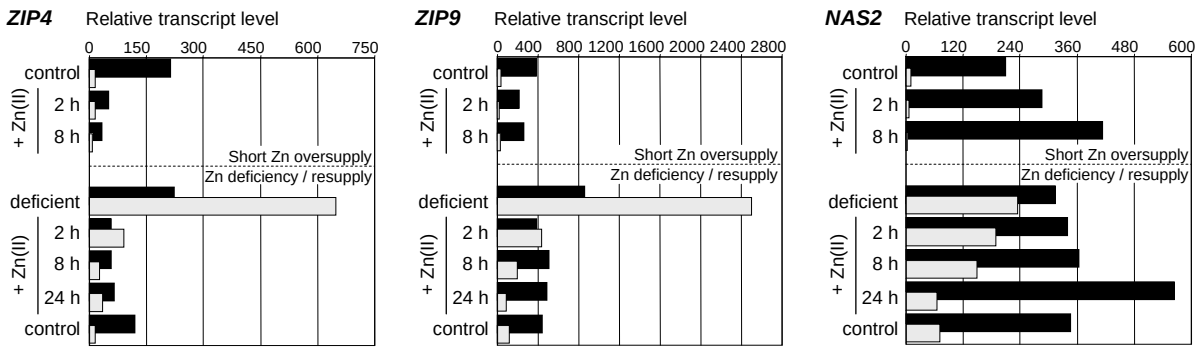

Shoot transcript levels

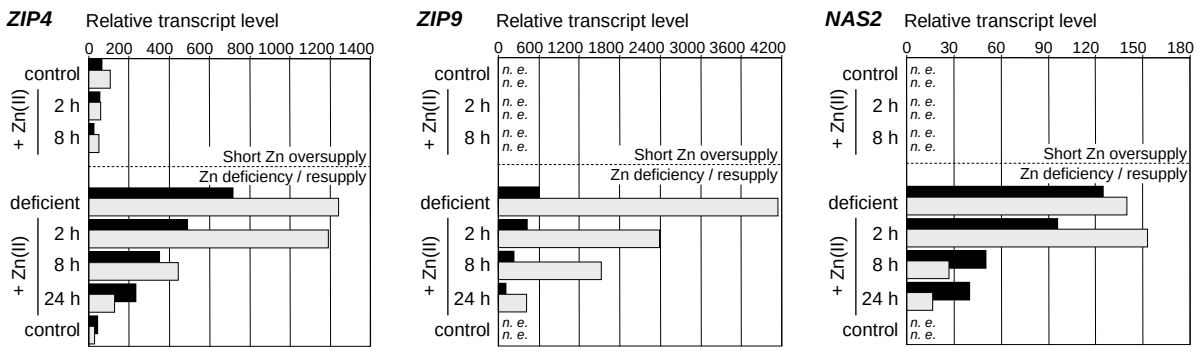

■ *A. halleri* □ *A. thaliana*

Figure 2 – Talke *et al.*

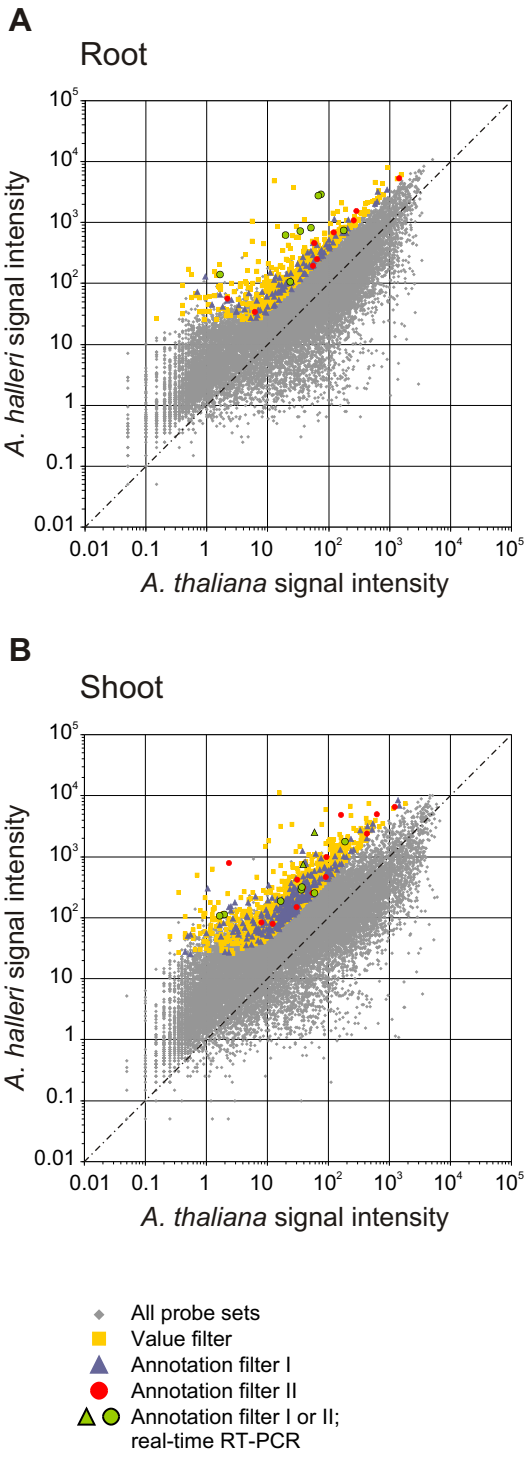

Figure 3 - Talke *et. al.*

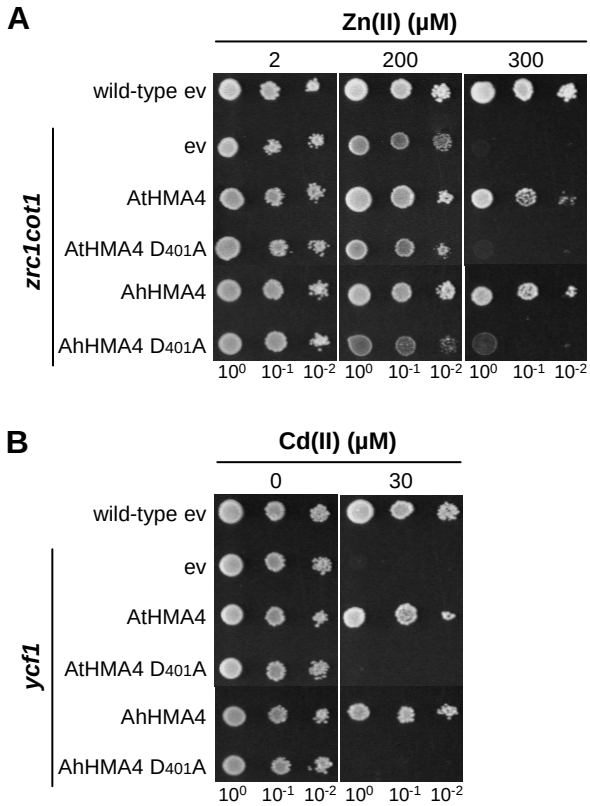

Figure 4 – Talke *et al.*

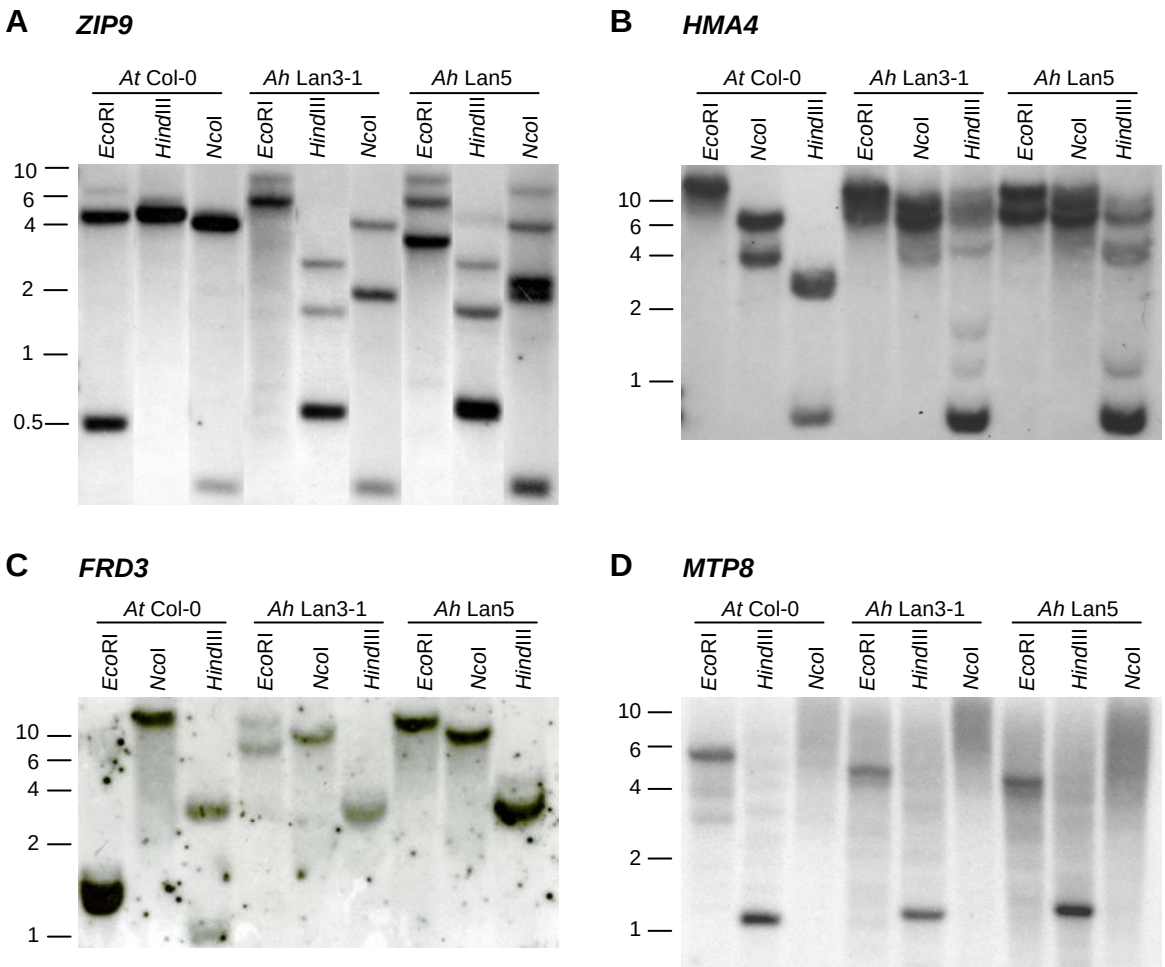

Figure 5 – Talke *et al.*

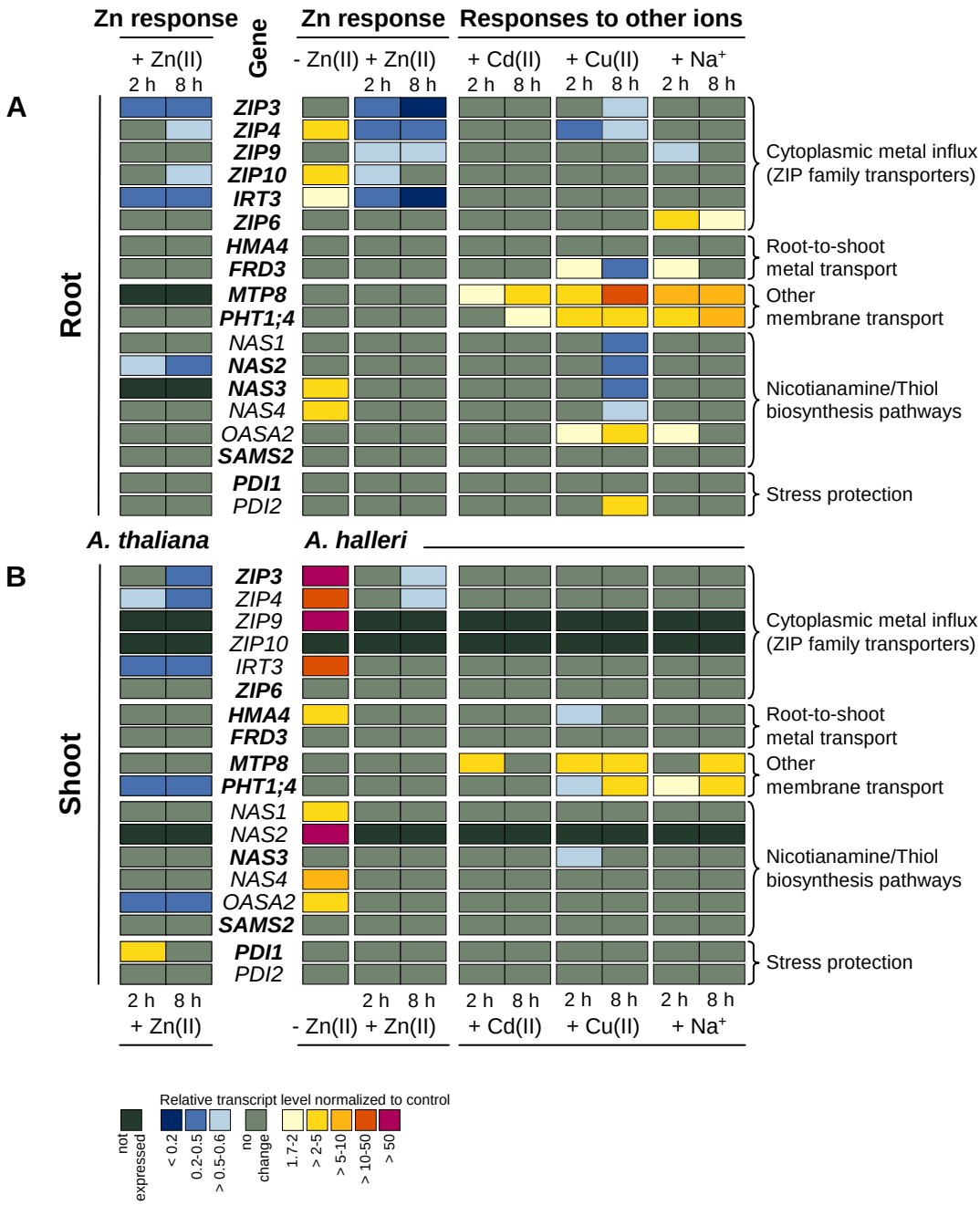

Figure 6 – Talke *et al.*

Root transcript levels

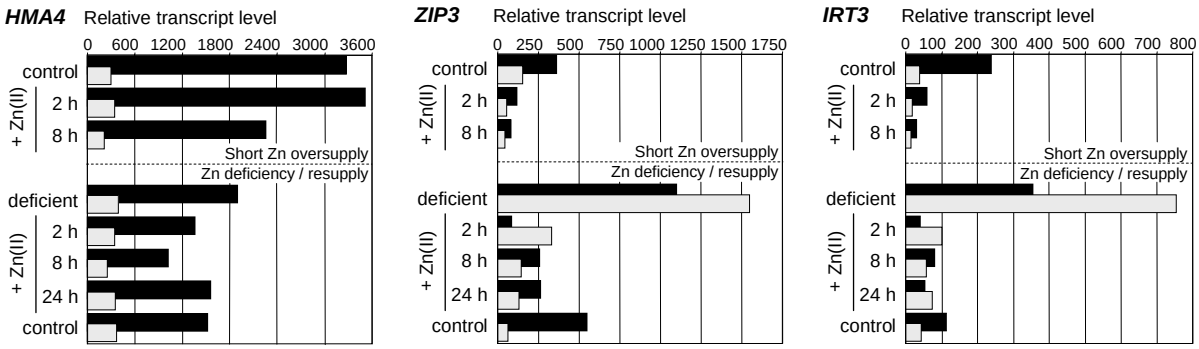

Shoot transcript levels

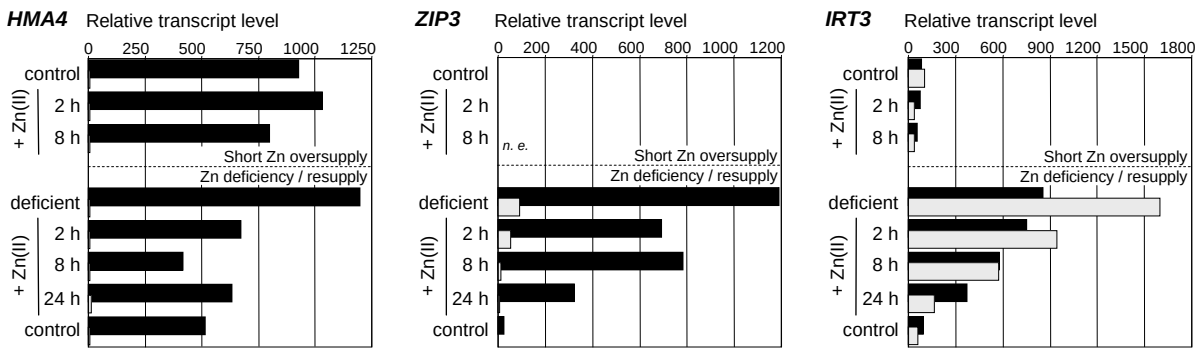

■ *A. halleri* □ *A. thaliana*

Figure 7 – Talke *et al.*

Supplemental Table IX. Sequences and reaction efficiencies of primer pairs used for real-time RT-PCR

Gene	*A. halleri* forward 5'-3'	*A. halleri* reverse 5'-3'	*A. halleri* reaction efficiency	Standard deviation RE	*A. thaliana* forward 5'-3'	*A. thaliana* reverse 5'-3'	*A. thaliana* reaction efficiency	Standard deviation RE
Ef1a	TGAGCACGCTCTTCTTGCTTTCA	GGTGGTGGCATCCATCTTGTTACA	1.945	0.025	identical pair		1.954	0.032
ZIP3	GGAGTTTTGAACGCTGCATCC	CTGCGAGAAAGTCCACCAGAGA	1.886	0.062	identical forward	CTGCGAGAAGGTCAACCAAAGA	1.854	0.037
ZIP4	AGCAAGAGAGGAATCAGGCTGC	CCAACCACGGGAACAACAGCA	1.880	0.040	AGCAAGAGAGGAATCAGGCTGC	CCAACCACAGGAACAACAGCA	1.857	0.034
ZIP9	CCATCACTACTCCCATCGGTGT	CACCAATGACGCAACGCTATAA	1.730	0.038	CCATCACTACTCCGATCGGTGT	CACCAATGCTGCAACGCTATAA	1.752	0.075
ZIP10	TTGCATCCTTCAGGCGGAGTA	CGCAAAAAAGAAAGCCATCACC	1.916	0.031	identical pair		1.873	0.072
IRT3	AGTCACCCTCCTGGTCATGGTT	GCCCATGCCCAATGTCAAT	1.860	0.047	AGTCATCCTCCTGGTCATGATT	GAGCATGACCAATGTCGAT	1.821	0.068
ZIP6	ATGGTGATATTTGCAGCCACC	CCTCCATTATCAATGCATTCG	1.863	0.073	ATGGTGATATTTGCAGCGACC	CCTCCATTATCAATGCGTTCG	1.878	0.041
HMA4	TGAAGGTGGTGGTGATTGCA	TCCACATTGCCCAACTTCG	1.888	0.064	AGAGAGCACGAATTGTTCCACG	GCCTGATACCACCAAGCTAGCA	1.850	0.041
FRD3	TGTGGCAGAGGAAGACACGAT	TCTGCATGAACAAGACTGGCTT	1.849	0.071	CGATATTCCCACTTGTGAGCC	TTCTCCATCGTGTCTTCCTCTG	1.827	0.071
MTP8	TCATCATTTTCGCCGCTGTT	CAATTGCTCAGCTGCCACAA	1.881	0.042	identical pair		1.845	0.051
PHT1;4	TCAAAGGAATTCATGAGTCGCC	GGAACCATGTCGATGTAGTGCC	1.864	0.051	identical pair		1.841	0.068
NAS1	CATGATCTTCCACACAACGGAC	CGACGTCATATTGGTCAAGGC	1.871	0.043	identical pair		1.918	0.032
NAS2	CCGATGATGTGGTTAATTCGG	TGCCTCGAGCTCCATTTGA	1.930	0.046	CTGACGACGTGGTTAATTCGG	TGCCTCGAGCTCCATTTGA	1.921	0.035
NAS3	ACGAACAATTGGTGCAAACA	GAGAATGTTGACATCTTCGG	1.854	0.059	identical pair		1.892	0.039
NAS4	ACGACCAACTCGTAAACAAG	GAGAGTGTCGACATCTTCAC	1.868	0.057	identical pair		1.905	0.042
OASA2	GCCTGTTGAAAGCCCTATTCTT	TGCCTGGAATAAAGCCAGCAC	1.900	0.050	GCCTGTTGAAAGCCCTATTCTG	TGCCTGGAATAAAACCAGCAC	1.838	0.042
SAMS2	GGAACACGTGATTAAGCCAATC	GGTTAAGGTGGAAGATGGTTTTG	1.919	0.029	GGAGCATGTGATCAAACCAATC	GGTTGAGGTGGAAGATGGTTTTG	1.927	0.033
PDI1	CCCCGTGGAGAGTCATCTGTAA	CTCCAGAGCTTCACCATCGAAA	1.902	0.041	identical pair		1.898	0.043
PDI2	TTCCTCGTGGAGAGTCTGTGGA	TCTCTAGAGCTTCCCCATTGAAG	1.882	0.074	identical pair		1.845	0.067

RE = reaction efficiency

Supplemental Table X. List of primers used for cDNA cloning and directed mutagenesis.

The CACC overhangs for cloning into the pENTR directional TOPO vector (Invitrogen) are underlined. The mutagenic bases in *HMA4* primers are shaded in grey.

Forward primers 5´-3´		**Reverse primers 5´-3´**		**Amplicon length (bp)**
ZIP3.F	ATAGCCGGCATAATCGGAGTTCT	ZIP3.R	GGCCATAATTTGAAGCCCAGTAT	775
ZIP4.F	TTCTTCTACCACTAAAATCCT	ZIP4.R	CATATGTCCGTGTGAATGT	622
ZIP6.F	ATGGCTTCTTGCGTCACC	ZIP6.R	CTAAGCCCAAAGAGCAAGTAGTG	1021
ZIP9.F	AGCATCACCGTCATAGCCTCT	ZIP9.R	AGATCCACGCGGGGTTAGTCT	311
ZIP10.F	AAGATGACTAAATCTCATG	ZIP10.R	CTTTAATTGAAGCTTGATGCTC	1022
IRT3.F	CAAAGTCTCTCTCAGCAACAG	IRT3.R	GGCTGAGAGCGAGTCCAAGATA	410
HMA4.F	CCGTGATTGTTGTTCACGACAG	HMA4.R	GAAATGCTTCGCCCGTTAAG	606
FRD3.F	GATCTATGACGGAAACTGGTGATG	FRD3.R	TGACTTTGTATCCGGAGCTGG	479
MTP8.F	GAAATGGAAGTCAATTATT	MTP8.R	TCTTCATAAATCGTTGGGGATT	1246
PHT1;4.F	ATGGTCATGGTCCTTTGTTCAATAGCC	PHT1;4.R	GTCCAGTGGTTGTAAGGAATAGCCAG	550
PDI1.F	TTTCCCTAAACTATCTGGCTCC	PDI1.R	CAGGTATTTCTTGTCGTCAGCA	514
PDI2.F	AGAGTTGAGTAGTCATAACCCTCCTCT	PDI2.R	ATGAGAAGTTGGCTTCTTCTCAC	1241
SAMS2.F	CAGGAAGAATGGAACTTGCCG	SAMS2.R	CATGCCATTAGCCACCACA	430
flAtHMA4.F	CACCCCGAAAATGGCGTTACAAAACAAAG	flHMA4.R	TCAAGCACTCACATGGTGATGGTG	3519
flAhHMA4.F	CACCCCGAAAATGGCGTCACAAAACAAAG	flHMA4.R	TCAAGCACTCACATGGTGATGGTG	3492
AtHMA4DA.F	CAAGATTGTTGCTTTCGCTAAAACTGGGACTATTACAAGAGGAG	AtHMA4DA.R	CTCCTCTTGTAATAGTCCCAGTTTTAGCGAAAGCAACAATCTTG	/
AhHMA4DA.F	AATCGCTGCTTTCGCCAAAACCGGGACTATTACCAGAG	AhHMA4DA.R	CTCTGGTAATAGTCCCGGTTTTGGCGAAAGCAGCGATT	/

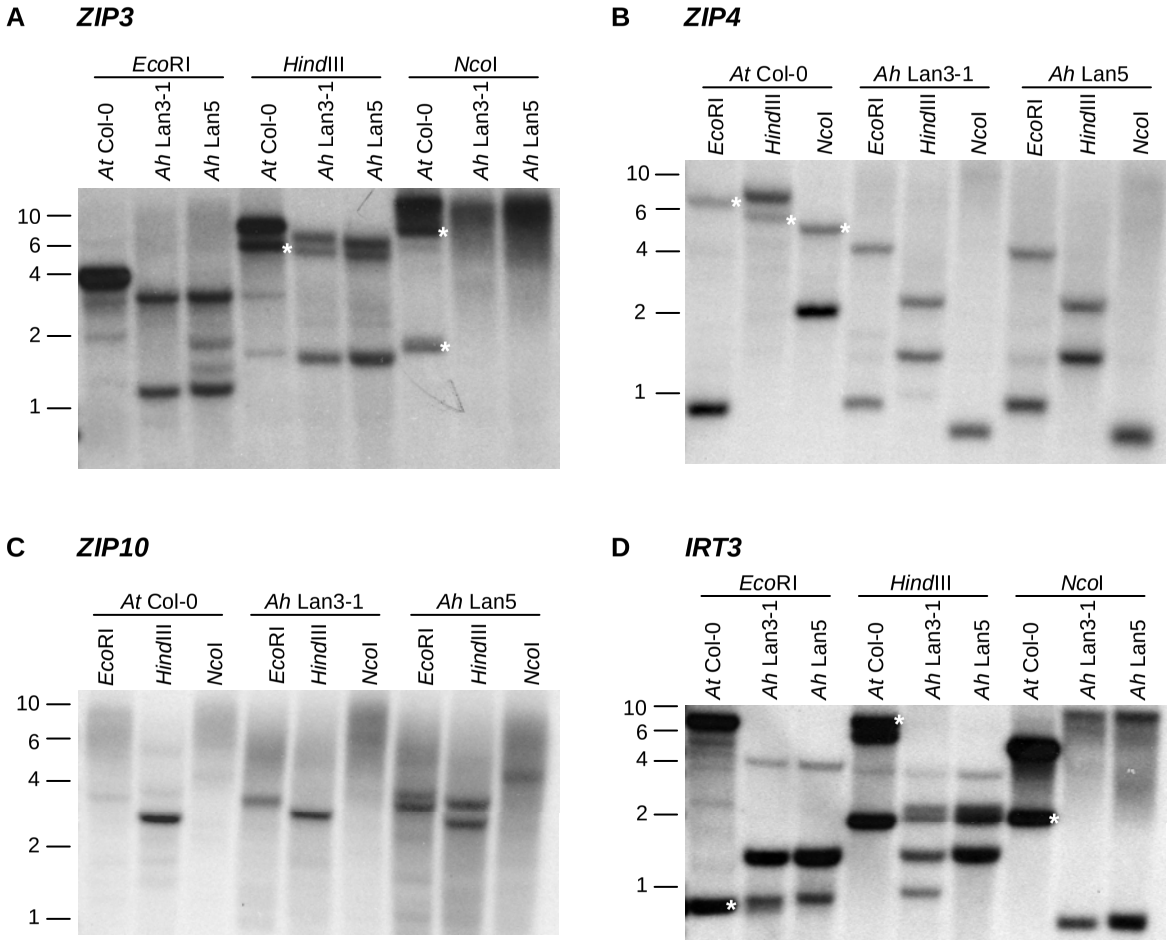

Supplemental Figure 1 (PartI)

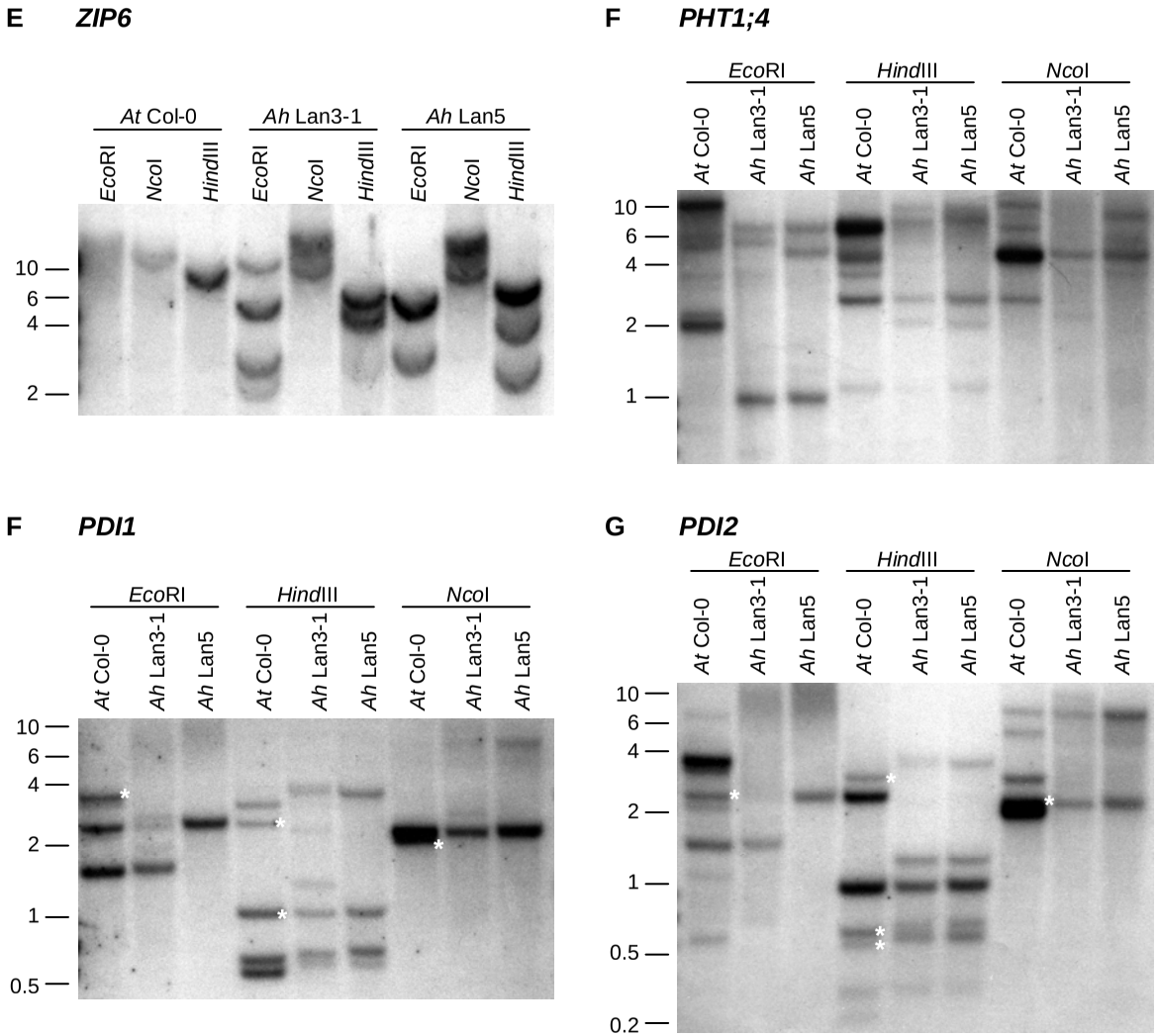

Supplemental Figure 1 (PartII)